THE DEVELOPMENT OF A HYDRAULIC EXCITER FOR THE INVESTIGATION OF MACHINE TOOLS

A. C. H. VAN DER WOLF

THE DEVELOPMENT OF A HYDRAULIC EXCITER
FOR THE INVESTIGATION OF MACHINE TOOLS

THE DEVELOPMENT OF A

HYDRAULIC EXCITER FOR THE

INVESTIGATION

OF MACHINE TOOLS

DOOR

ANTONIUS· CORNELIS HERMANUS VAN DER WOLF

GEBOREN TE BREDA

Dit proefschrift is goedgekeurd door de promotor

PROF. IR. C. DE BEER

aan mijn ouders
aan Carla

CONTENTS

I. INTRODUCTION

1.1. Background of the problem

During the machining of metals periodic forces will appear in the circuit consisting of machine tool, workpiece and cutting tool. These forces are generated by the process itself. Owing to this a relative motion between workpiece and cutting tool may arise increasing the periodic forces. Eventually the tool gets into a stationary vibration. This so-called "chatter" vibration influences the cutting process in a very unfavourable way. It decreases the shape and dimension accuracy of the workpiece and it also impairs the quality of the machined surface. Furthermore, chatter may shorten tool life and causes smaller chip production of the machine tool.

After World War II a great number of papers on this phenomenon have been published. The first fundamental work was done by ARNOLD (1). He carried out his experiments under extreme conditions (stiff workpiece, flexible tool and a rigid lathe) and found that chatter is mainly the result of the cutting force as a function of the cutting speed showing a falling characteristic. HAHN (2) has shown that dynamic instability can also be observed in materials which do not have a falling cutting force characteristic. DOI and KATO (3) have found that the chip-thickness variation is also important to the chatter phenomenon. They regard the time delay between the chip-thickness variation and the cutting-force variation as a fundamental effect.

Another viewpoint is held by TOBIAS and FISHWICK (4), (5). They assume that the dynamic cutting-force variation dP is a function of three independent factors and can be expressed as

$$dP = k_1 ds + k_2 dr + k_3 dv \qquad (1.1)$$

Except for the already mentioned variables s (chip thickness) and v (cutting speed), they also consider the feed rate r as a major quantity with respect to the cutting-force variation. The values for k_1, k_2 and k_3 can only be found by dynamic experiments. TOBIAS and FISHWICK **9**

used this cutting-force variation dP to solve the differential equation of an elementary vibratory system (the tool). In this way they found a stability chart with stable and unstable regions.

The contribution of the Czech investigators TLUSTY, POLACEK, DANEK and SPACEK (6) to the solution of the chatter problem starts from a simple force relation

$$dP = k'ds \tag{1.2}$$

and a vibrating system of two degrees of freedom. They distinguish two causes of the chatter phenomenon

— the "mode-coupling" effect, which arises from two vibra-
ting directions resulting in an elliptic path of the tool
point

— the "regenerative" effect, which comes from a chip-thick-
ness variation when the surface of the work has already
been cut during a preceding machining operation on the
work.

In both cases they solved the equations of motion and found a stabi-
lity chart. Furthermore, they determined a minimum value of the cut-
ting-force coefficient k'_{min} at which instability may occur.

A completely graphical solution of the problem by PETERS and VANHERCK (7) is of surprising simplicity. Although, their method is not quite new (8), (9), they succeeded in combining all theories about chatter offered up to now. They used the block diagram as shown in fig. 1.1.
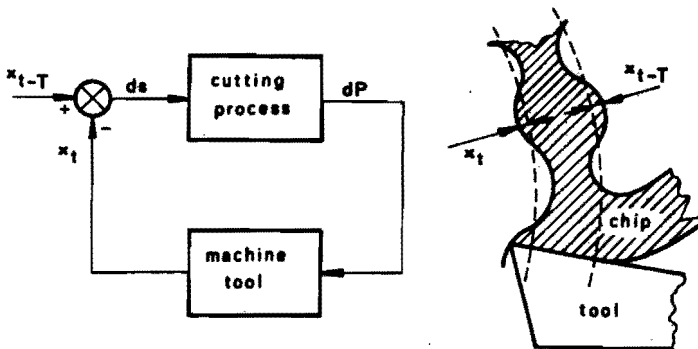
10 Fig.1.1. Block diagram of chatter loop

Besides Eq. (1.2) mentioned above, they used

$$ds = \mu x_{t-T} - x_t \qquad (1.3)$$

When overlapping factor $\mu = 1$, Eq. (1.3) yields

$$ds = x_{t-T} - x_t \qquad (1.4)$$

By considering the transfer functions of the cutting process and the
machine tool, it requires no more than some simple constructions to
find a minimum value of k', as did TLUSTY, POLACEK, DANEK and SPACEK
(6). In this context it is obvious that the last named investigators
studied more especially the transfer function of the machine tool,
whereas TOBIAS and FISHWICK (4), (5) studied that of the cutting pro-
cess. It is obvious that in the theories mentioned above the transfer
function of the machine tool has to be known. In general it is neces-
sary to use an experimental method to determine this transfer func-
tion.

The method of PETERS and VANHERCK has been generally accepted (10),
(11), (12).

1.2. Review of the problem

To determine the dynamic qualities of a machine tool an exciter is
required enabling a harmonic force-variation to be introduced into
the element to be investigated. The frequency of this dynamic force
has to be adjustable. Because generally the machine tool consists of
non-linear elements, it will often be necessary to introduce a static
force, too. In this way the load of the machine tool during the cut-
ting process can be imitated.

Up to now electro-dynamic exciters have often been used (Goodman,
Philips). However, these exciters have some disadvantages, such as
proportionately large dimensions and mass of the exciter when great
dynamic forces have to be obtained. Furthermore, electro-dynamic
exciters cannot give static forces of any magnitude.

The latest developments, of which ref. (13) gives an excellent sur-
vey, try to eliminate these disadvantages. As an example, the elec-
tro-hydraulic exciter (10), (14) may be mentioned.

In the Laboratory of Production Engineering (Department of Mechanical
Engineering) at the Technological University at Eindhoven a new type   **11**

of hydraulic exciter has been developed, which meets the following requirements

-- dimensions: 50 mm x 35 mm in dia.

-- total mass: 350 g

-- frequency range: 10 ÷ 1000 Hz

-- dynamic force: amplitude adjustable up to 300 N

-- static force: adjustable up to 3000 N.

The pressure waves in the hydraulic system are created by a simple mechanically driven valve. This is the most characteristic difference between the Eindhoven exciter and those mentioned in refs. (10) and (14). The latter work with the aid of an electro-hydraulic servo-valve. Lastly, the question remains how to record the response of the element that has been excited. Although a Bode-diagram gives more information, a Nyquist-diagram is generally used. In this way the data are immediately available for the graphical solution of PETERS and VANHERCK (7).

A theoretical and experimental study about the hydraulic exciter mentioned will be described in the following chapters.

2. TECHNICAL EQUIPMENT OF THE EXCITER PLANT ·

2.1. Introduction

Fig. 2.1 shows the exciter plant diagrammatically.

A vane pump supplies the oil quantity to the hydraulic circuit. The
pump is driven by a three-phase motor.
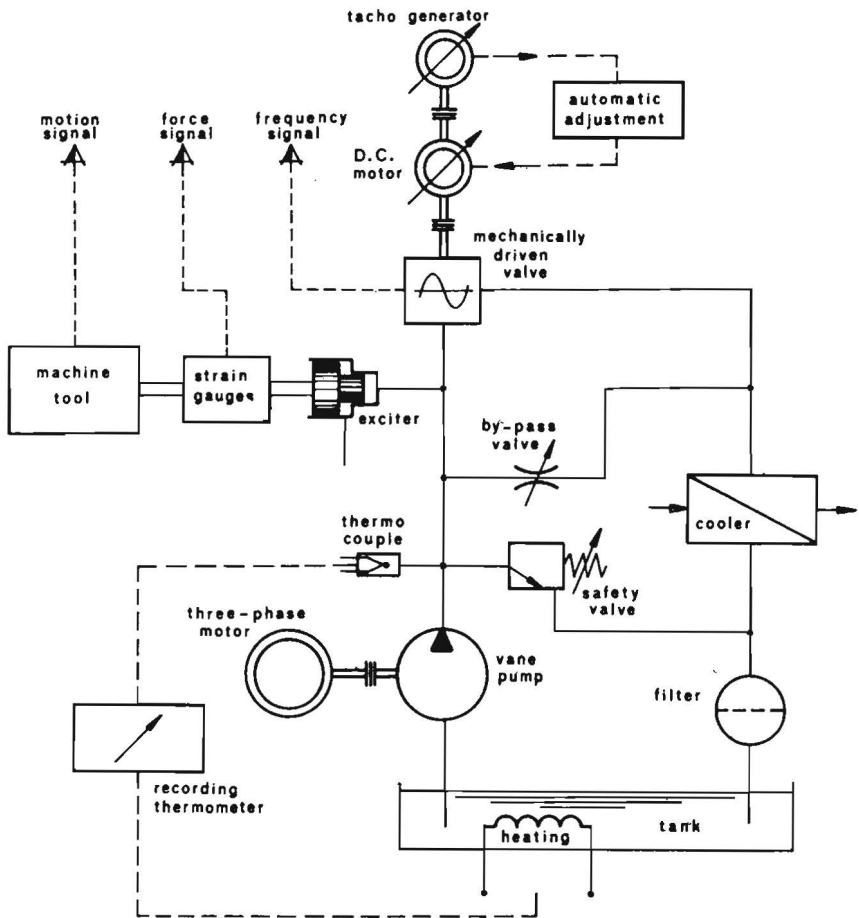
Fig.2.1. The exciter plant

After passing through a mechanically driven valve, which creates a
sine-shaped pressure in the hydraulic system, the oil flows back to
the tank via a cooler and a filter. A D.C. motor, with automatic ad-
justment of the speed of rotation, drives the valve.
Further, there is an exciter which forms the link between the oil sys-
tem and the machine tool. The force introduced into the machine tool
by the exciter, can be measured by way of strain gauges.
Pipes connect the several elements of the oil system.
In addition to an automatic temperature control for the oil, the exci-
ter plant has a safety valve to limit the maximum oil pressure. Lastly,
there is a by-pass valve for starting the system at no-load.
The major parts of the exciter plant will now be discussed separately.

2.2. The vane pump

A requirement which the pump should answer for the hydraulic system,
is that it delivers a constant flow of oil independent of the pressure
in the system. Further, the pressure signal should show little noise.
Gear pumps and piston pumps are less suitable for this purpose. Al-
though, a screw pump is also satisfactory, an ordinary type of vane
pump (Ate) was chosen. Fig. 2.2 gives a view of the inside of the pump.
There are nine cells in the pump and two outlet ports.
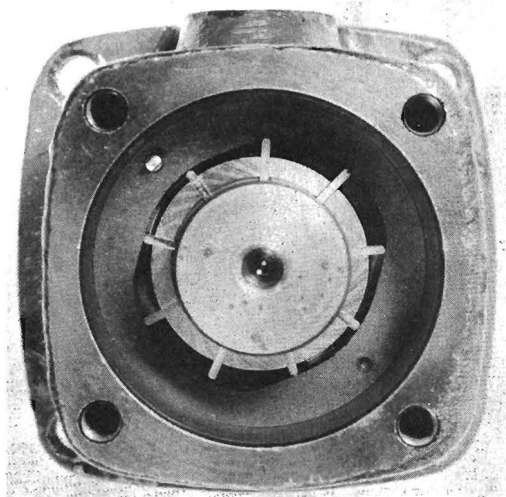
14 Fig.2.2. The vane pump with the front removed

The nominal speed of rotation of the pump shaft is 50 Hz (frequency of
the mains voltage).

The delivery of the pump Q in a small measure depends on the pressure
p in the outlet of the pump, and can be expressed as

$$Q = 0.226 \times 10^{-3} - 3.10 \times 10^{-12} \, p \qquad (2.1)$$

This relation, valid in the range $0 < p < 70 \times 10^5$ N/m^2, was determi-
ned with the aid of a flow meter (Gloster Equipment Ltd.) and an in-
ductive pressure-transducer (Vibro-meter) for 50 $^\circ$C temperature of the
fluid medium (Mobil Oil DTE Medium). The pressure in the inlet of the
pump was neglected. The inaccuracy in the determination of the flow Q
may be estimated to be $\pm$ 1%. The maximum slip of the speed of rotation
of the pump shaft in respect of the mains frequency is 2% at
$p = 70 \times 10^5$ N/m^2.

The noise of the pressure signal of the vane pump was also determined
by an experimental method. With the aid of a quartz pressure-transdu-
cer (Vibro-meter) the noise was made visible. Fig. 2.3 represents the
corresponding graph for a pressure $p = 35 \times 10^5$ N/m^2.
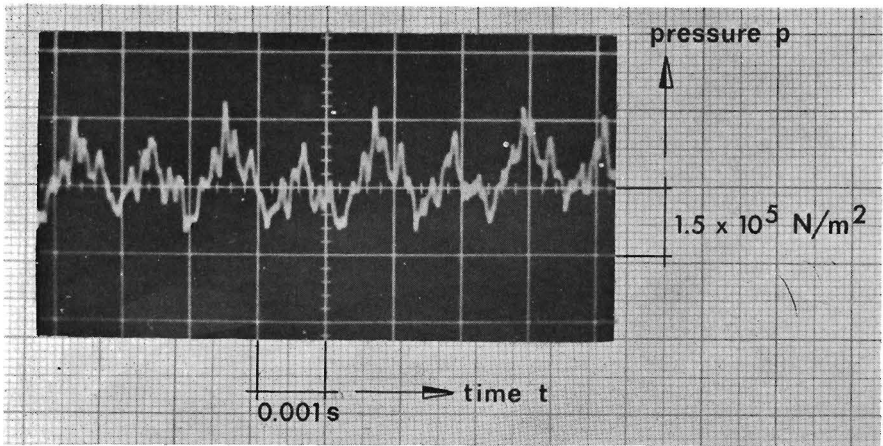
Fig.2.3. Noise of the pressure signal

In this photograph can be distinguished a frequency of 900 Hz due to
the combination of the speed of rotation of the pump shaft (50 Hz),
the two outlet ports, and the nine vanes. Even the difference between
the two outlet ports resulting in a frequency of 450 Hz can be seen. **15**

The half peak-to-peak value of the noise is small and is 3.5% of the value of p. In the cases where it is important (Chap. 3), a correction for this noise signal will be introduced.

2.3. The mechanically driven valve

2.3.1. Valve construction

The idea of a rotary-piston valve, which forms the basis for the construction, is not quite new. This valve construction has already been applied in milking machines (15) and in equipment for fatigue tests (16). It has to be noticed that in all those applications the valve is used for low frequencies only (up to 50 Hz).
The design of the valve is given in fig. 2.4. The high-pressure pipe A connects the valve block B and the pump. The oil flows from the
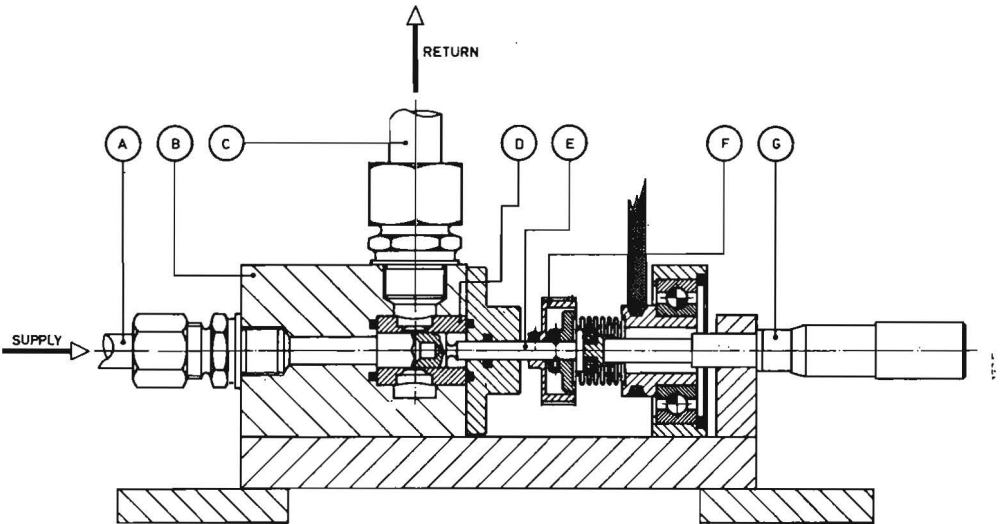
Fig.2.4. The mechanically driven valve

high-pressure side of the valve block to the return pipe C through two slit-shaped orifices in cylinder D. The area of the orifices is determined by the position (axial and radial) and the shape of the piston E.
Piston E is driven by a V-belt. The number of revolutions can be measured with the aid of toothed wheel F. Micrometer G adjusts the axial position of piston E.

16 Fig. 2.5 shows a photograph of the cylinder and two pistons.
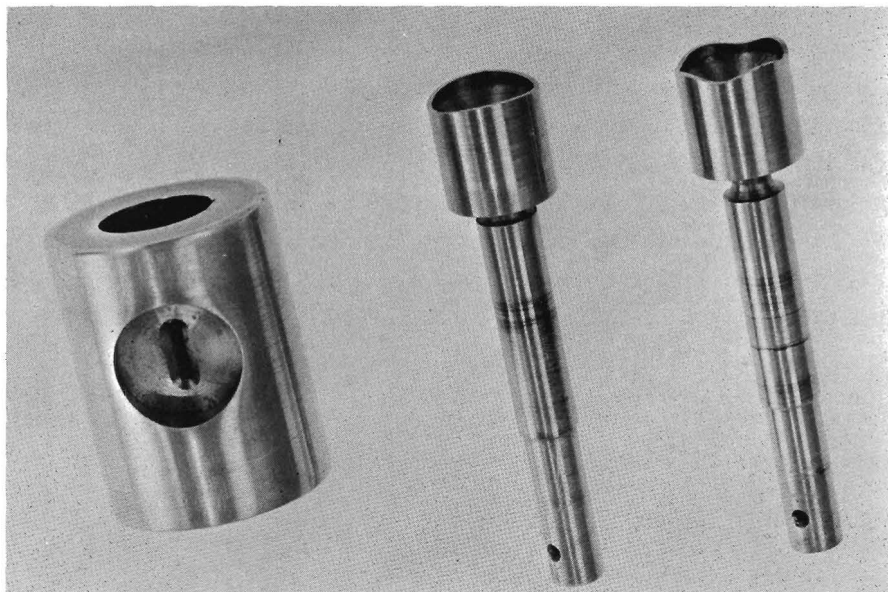
Fig.2.5. Cylinder and two pistons
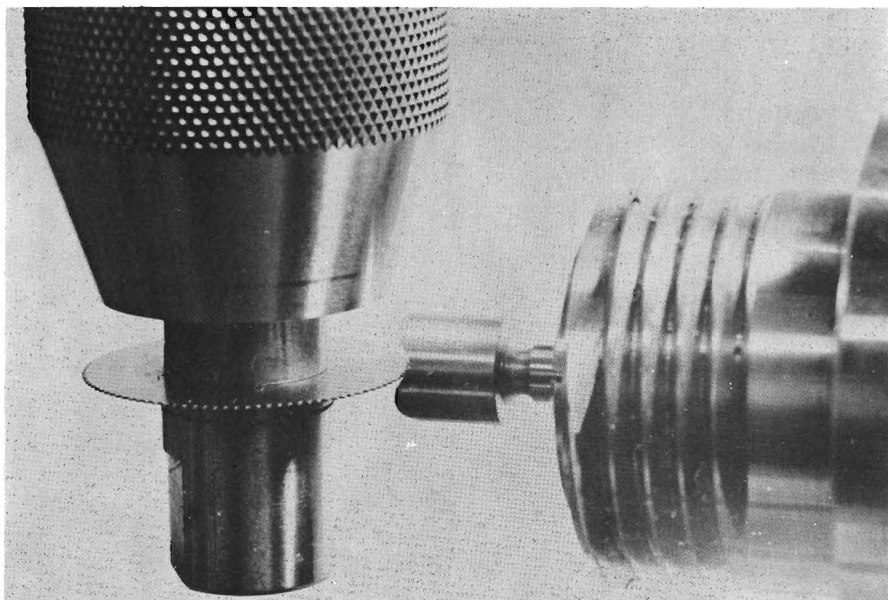
Fig.2.6. The machining of the piston

All parts of the valve were made in the Laboratory of Production En-
gineering at the Technological University at Eindhoven. The making
of the piston E required very special care with a view to correct
functioning of the valve. A SGIP jig-boring machine was used to give
the rim of the piston a very accurate and particular shape.
As shown in fig. 2.6 a very thin metal slitting saw machined the rim
of the piston until the correct axial measure going with a certain
radial coordinate of the piston was reached. The radial position of
the piston can be changed with a dividing head. Two hundred and eigh-
ty radial adjustments of the piston are required to give the rim of
the piston the correct shape.

2.3.2. Drive of the valve

As already mentioned in Sec. 2.1 the valve is driven by a D.C. motor.
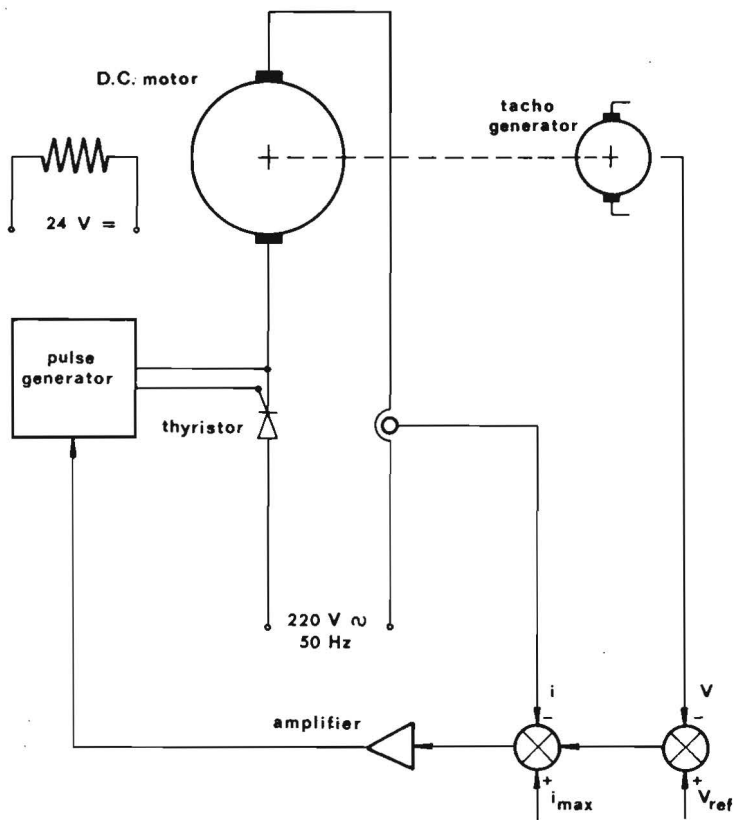
18   Fig.2.7. Automatic control of the speed of rotation of the D.C. motor

Provision has to be made for very accurate adjustment of the speed of rotation of the valve. Afterwards, during the experiment the adjusted value should be kept constant. For this reason the automatic control arrangement of fig. 2.7 has been designed.

The D.C. motor working with independent direct-current field excitation (24 V), is mechanically coupled with a tacho generator. The output of this generator is a voltage V proportional to the speed of rotation of the D.C. motor. The difference between V and a pre-set voltage V_{ref} is led to an amplifier.

If $V < V_{ref}$ the output voltage of the amplifier controls the pulse generator. The latter supplies the thyristor with pulses (repetition frequency 50 Hz). The thyristor is fired by every one pulse and stops operating when the voltage becomes zero (see fig. 2.8). The thyristor is connected in series with the armature of the D.C. motor.
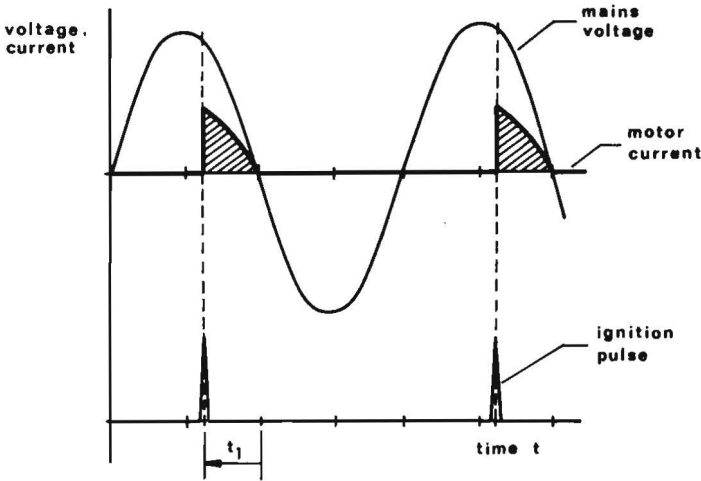
Fig.2.8. Voltage and current diagram of the thyristor circuit

The hatched area in fig. 2.8 is proportional to the average motor-current, which is determined by the time t_1. This time t_1 depends on the magnitude of the input of the pulse generator. In reality, the thyristor circuit is carried out double-acting, by which both half-periods of the voltage in fig. 2.8 can be utilized.

If $V > V_{ref}$ the D.C. motor is disconnected from the mains and operates as a generator to get rid of the surplus of energy.

19

With the aid of this control unit, which has been applied in driving engineering of late years (17), it is possible to keep constant the speed of rotation of the valve at $\pm$ 0.1 Hz.

2.3.3. Characteristic equation of the valve

The valve as described in Sec. 2.3.1 follows the orifice equation

$$Q = C A \sqrt{\frac{2\Delta p}{\rho}} \qquad (2.2)$$

The rate of flow Q is delivered by the pump (see Sec. 2.2). Assuming no pressure drop in the connecting pipe between pump and valve, we can combine Eqs. (2.1) and (2.2) to find an expression for the orifice area

$$A = \frac{(0.226 \times 10^{-3} - 3.10 \times 10^{-12} \ p) \sqrt{\rho}}{C \sqrt{2\Delta p}} \qquad (2.3)$$

Using the same conditions as we have done for the determination of Eq. (2.1), it is possible, as a result of an experiment, to describe the pressure drop in this particular case as

$$\Delta p = p - 1.75 \times 10^5 \qquad (2.4)$$

where p = pressure before the valve orifice.

In Eq. (2.4) the maximum error in Δp for $p > 10 \times 10^5$ N/m^2 may be fixed at $\pm$ 1%.

In the same way the experimental relationship between C and p has been determined, viz.,

$$C = 0.665 + 0.017 \times 10^{-6} \ p \qquad (2.5)$$

where the inaccuracy of C can be assumed to be $\pm$ 2%.

After substituting Eqs. (2.4) and (2.5) in Eq. (2.3) and using for ρ the density of the applied fluid medium (ρ = 856.2 kg/m^3 for 50 $^\circ$C), we find

$$A = \frac{(6.613 \times 10^{-3} - 0.091 \times 10^{-9} \ p)}{(0.665 + 0.017 \times 10^{-6} \ p) \sqrt{2p - 3.5 \times 10^5}} \qquad (2.6)$$

With Eq. (2.6) it is possible to calculate the area A for every wanted value of p. It needs hardly be observed that the results of these calculations are only valid in the particular circumstances mentioned before.

20

2.3.4. Distortion of the pressure signal

Let us assume that the pressure p, in accordance with what has been mentioned in Sec. 1.2 , consists of a static part b_0 and a dynamic part b_1 cos ωt as

$$p = b_0 + b_1 \cos \omega t \qquad (2.7)$$

If Eq. (2.7) is combined with Eq. (2.6) we find the area A as a function of ωt, provided the numerical values of b_0 and b_1 are given. It is obvious that A also consists of a static and a dynamic part. The static part A_{stat} determines the axial position of the piston E in the cylinder D, because the two slit-shaped orifices in the cylinder have a given area (see fig. 2.4). The shape of the rim of the piston E is given by the dynamic part A_{dyn}.
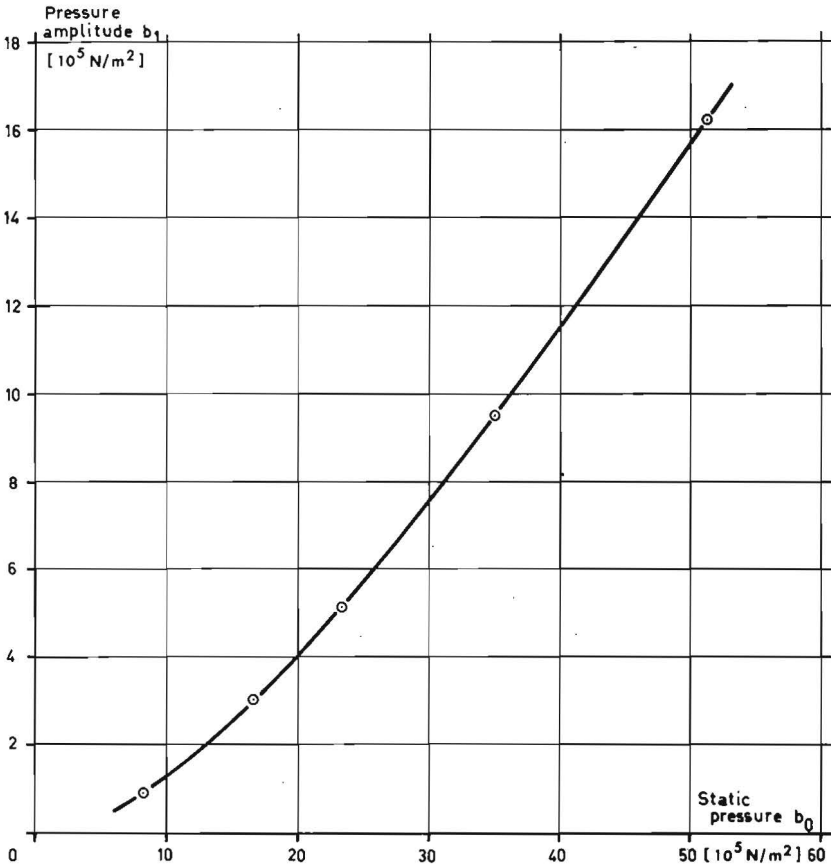
Fig.2.9. Pressure amplitude b_1 as a function of static pressure b_0

When designing the valve with the aid of this calculation, it is possible to choose, in addition to the calculated value A_{stat}, other values for A_{stat} in combination with the already calculated value of A_{dyn}. In that case, it is important to know the distortion of the pressure signal. Because the area A is an even function of ωt the pressure p can be generally described as

$$p = b_0 + b_1 \cos \omega t + b_2 \cos 2\omega t \ldots .+ b_n \cos n\omega t \quad (2.8)$$

The coefficients $b_2, \ldots \ldots, b_n$ give an idea of the distortion of the pressure signal.

A great number of valves has been designed and analysed in the way referred to, using the IBM-1620 digital computer [*]. A representative example will be discussed now. The results of the calculation can be seen in figs. 2.9 and 2.10.
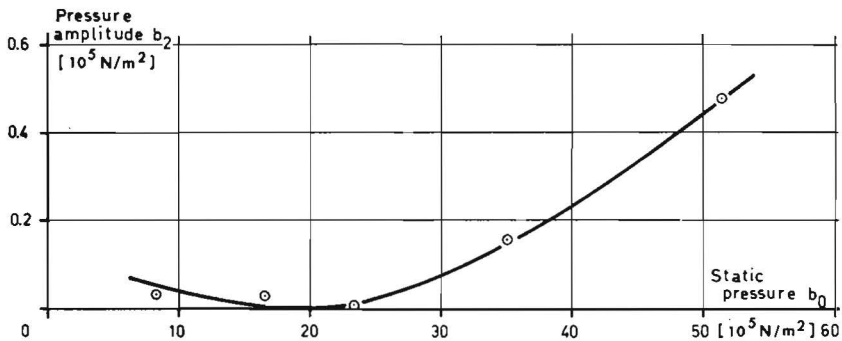
Fig.2.10. Pressure amplitude b_2 as a function of static pressure b_0

The first graph shows b_1 as a function of the static pressure b_0. The valve was originally designed for a static pressure of about 20×10^5 N/m^2. Of course, at this point the magnitude of b_2 is equal to zero (see fig.2.10). Furthermore, we can see that the value of b_2 is small with respect to b_1 (max. 3.3%). The coefficients b_3, b_4, b_5 and b_6 have been calculated too, but they are negligibly small. The calculation shows that this valve can be used in a wide range of static pressures with little distortion.

22 [*] Data may be obtained on request.

2.4. The exciter

Some specifications of the exciter have already been mentioned in
Sec. 1.2. Fig. 2.11 shows that the exciter has been carried out as a
longitudinal one.
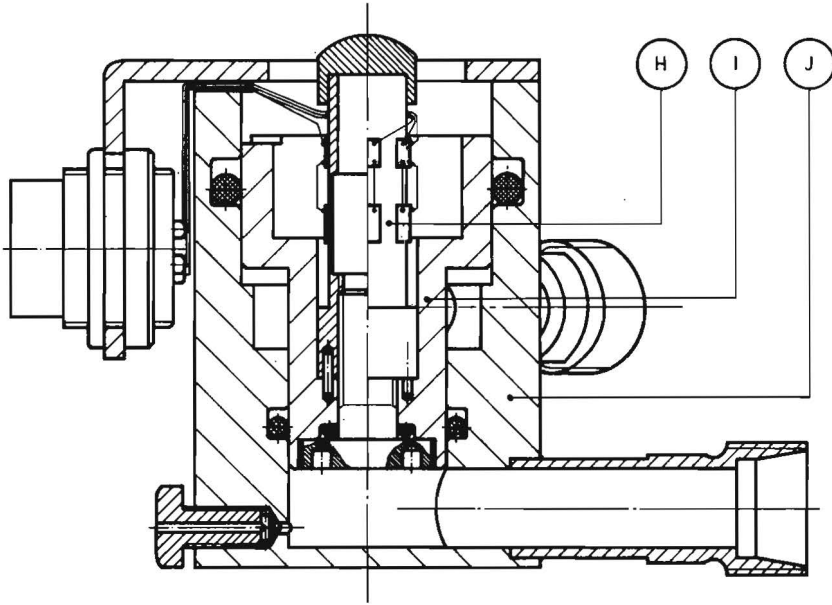
Fig.2.11. The exciter

The piston I is mounted in a chamber J. The oil can actuate the pis-
ton by means of two active surfaces, which can be used at choice.
The circular surface has an area of about 200 mm^2, the annular sur-
face one of about 300 mm^2. The link between the piston I and the ma-
chine-tool part to be investigated is formed by a measuring element
H. Strain gauges are glued on it to measure static and dynamic for-
ces in a range from 1 up to 4000 N. The mass of piston and measuring
element together is about 100 g.
The dimensions and mass of this exciter are small in comparison with
other exciters (see ref. (13)). Therefore the Eindhoven exciter is
pre-eminently suited to the investigation of smaller machine tools.
However, the forces this exciter can deliver make it also suitable

23

for use on medium-type machine-tools. Fig. 2.12 shows a photograph
of the exciter.

Fig.2.12. Photograph of the exciter

2.5. Summary

In the first stage of our investigation we tried to explain the pro-
perties of the hydraulic high-pressure system on the basis of the e-
quations of pump and valve such as they are described in the present
chapter. As a matter of fact this method of calculation was based on
the assumption of incompressibility of the oil, which is not unusual
in designing hydraulic exciters (see ref. (14)). As can be read in
ref. (18), testing of a prototype revealed that the calculation only
satisfied lower frequencies. The percentages of distortion, as cal-
culated in Sec. 2.3.4 turned out to be correct.
Then a model was designed taking into account the compressibility of
the oil. In this model the behaviour of the hydraulic system is
mainly determined by the oil-filled pipes connecting the several e-
lements. The characteristics of pump and valve are now only boundary
conditions of the problem as is the motion of the piston of the ex-
24 citer. In Chap. 3 this model will be amply discussed.

3. AN ANALOGUE OF THE HYDRAULIC PLANT

3.1. Introduction

The analogue study, which is the subject of this chapter, is inten-
ded to make researches into the relationship between the pressure
amplitude b_1 and the frequency f. This pressure amplitude must be
kept constant in a certain frequency range during the investigation
of machine tools carried out with the aid of the hydraulic exciter.
In order to design the hydraulic plant as optimal as possible in
this respect, the influence of a great number of parameters has to
be known.
The study has been carried out with two models, which are diagram-
matically shown in fig. 3.1.

model A   model B
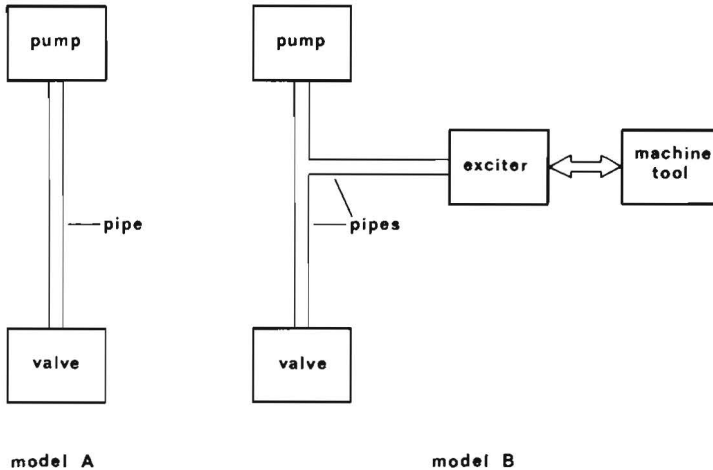
Fig.3.1. Two analogue models

Model A only consists of a pump and a valve connected by a pipe.
With the aid of this model the validity of such an analogue has

been tested by comparing the analogue solutions with experimental
results. The parameters, which are varied in this model are the mo-
dulus of elasticity of the fluid medium, the static pressure b_0,
the place of the point of observation on the pipe, and lastly the
length of the pipe between pump and valve.

Model B agrees with the total hydraulic plant. With this model va-
rious experiments on machine tools are simulated. In addition to
the length of the pipes the dynamic qualities of the machine tool
are varied in this model.

All computations are made on analogue computer PACE 231 R. The dis-
cussion of details of the analogue computations is beyond the scope
of this chapter, only main parts will be mentioned. Many ideas for
this analogue study originate from ROGERS and CONNOLLY (19); JACK-
SON's contribution (20) has also been consulted occasionally.

3.2. Model A

3.2.1. The analogue elements of the model

3.2.1.1. The pipe

We consider the uniform oil-filled pipe as a one-dimensional pro-
blem. For an unsteady, frictionless, compressible flow of this
kind the two basic equations are

$$- \frac{\partial v}{\partial x} = \frac{1}{E} \frac{\partial p}{\partial t} \tag{3.1}$$

$$- \frac{\partial p}{\partial x} = \rho \frac{\partial v}{\partial t} \tag{3.2}$$

This pair of simultaneous partial-differential equations is known
as the wave equations (see refs. (21), (22), (23)). It should be
noticed that E is not the modulus of elasticity of the liquid alo-
ne. The elasticity of the pipe has also to be taken into account.
We used seamless drawn piping with an inside diameter of 8 mm and a
thickness of the pipe wall of 1 mm. In this case a simple calcula-
tion will show that the elasticity of the steel pipe may be neglec-
ted with respect to the elasticity of the oil.

There is a general solution of the Eqs. (3.1) and (3.2), which makes
the problem analytically approachable (see ref. (24)).

26 Graphical methods have been used to solve the wave equations (see

refs. (22), (23)) in the case of sudden changes in a steady flow
(water-hammer effect).
The boundary conditions of our problem are non-linear relationships
between pressure p and velocity v in the case of valve and machine
tool. This makes the problem unsuitable for the treatment with ana-
lytical and graphical methods.
For the analogue computations we divide the pipe into segments of
length Δx as shown in fig. 3.2.
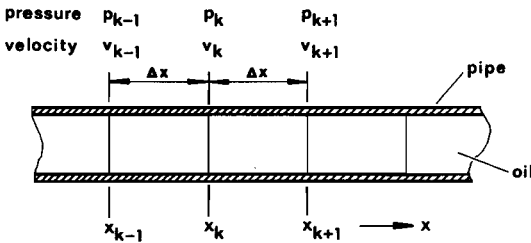
Fig.3.2. The pipe

Using the method of finite differences we only consider pressure and
velocity at discrete values of x. At the point x_k for example the
pressure is p_k and the velocity v_k. If the interval of x is divided
into n segments there are only (n+1) pair of values (p_k, v_k) availa-
ble. Scaling of the variables is necessary for the analogue computa-
tions. We assume

$$p_k^* = \frac{p_k}{p_m} \tag{3.3}$$

$$v_k^* = \frac{v_k}{v_m} \tag{3.4}$$

where p_m and v_m are the maximum values of pressure and velocity.
A change of time scale will also be necessary to slow down the speed
of solution. Therefore we introduce a computer time τ as

$$\tau = \beta t \tag{3.5}$$

where β is the time scale factor.
With the aid of a second-order finite-difference approximation for
the derivatives of pressure and velocity with respect to x, and the **27**

Eqs. (3.3), (3.4) and (3.5), the wave equations (3.1) and (3.2)
change into

$$\frac{d}{d\tau} (\overset{*}{p}_k) = - \frac{v_m \ E}{p_m \ \beta \ 2\Delta x} (\overset{*}{v}_{k+1} - \overset{*}{v}_{k-1}) \qquad (3.6)$$

$$\frac{d}{d\tau} (\overset{*}{v}_k) = - \frac{P_m}{v_m \ \beta \ 2\Delta x \ \rho} (\overset{*}{p}_{k+1} - \overset{*}{p}_{k-1}) \qquad (3.7)$$

where k = 1, 2, 3, ...,(n-1).

The analogue-computer circuit for the Eqs. (3.6) and (3.7) is given
in fig. 3.3.
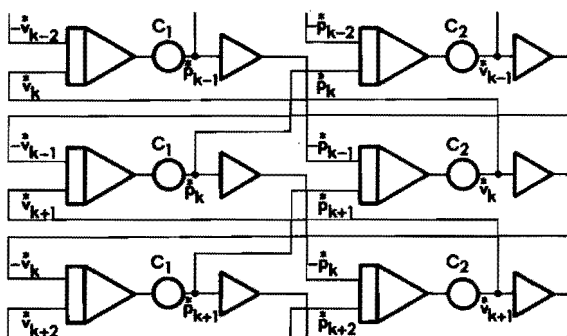
Fig.3.3. The analogue-computer circuit for solving the wave equations

The coefficients C_1 and C_2 represent the quotients of parameters
which are used in Eqs. (3.6) and (3.7) respectively, thus

$$C_1 = \frac{v_m \ E}{p_m \ \beta \ 2 \ \Delta x} \qquad (3.8)$$

$$C_2 = \frac{P_m}{v_m \ \beta \ 2\Delta x \ \rho} \qquad (3.9)$$

Numerical values of C_1 and C_2 can be adjusted in the computer cir-
cuit by means of potentiometers.

3.2.1.2. The pump

In order to introduce the boundary conditions into the analogue mo-
del, we use a method which is also applied to the model study of a

vibrating cantilever beam (see ref. (19), p. 182). We assume that
the pump is at point $x = x_{\frac{1}{2}}$ of the pipe (see fig. 3.4).
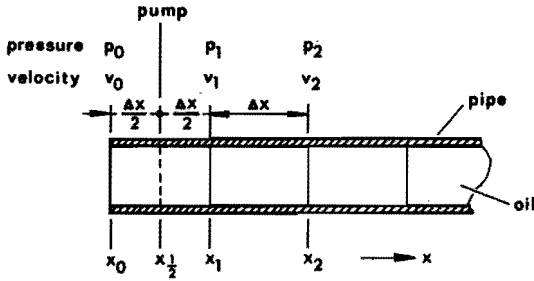
Fig.3.4. The pump end of the pipe

Pressure and velocity are not available at point $x = x_{\frac{1}{2}}$ (see Sec.
3.2.1.1). Therefore, we define

$$p_{\frac{1}{2}} = \frac{p_0 + p_1}{2} \tag{3.10}$$

$$v_0 = v_1 \tag{3.11}$$

$$v_{\frac{1}{2}} = v_1 \tag{3.12}$$

As boundary condition at $x = x_{\frac{1}{2}}$ we use Eq. (2.1) (see Sec. 2.2).
After dividing by the cross-sectional area of the pipe
(50.2×10^{-6} m^2) and scaling, Eq. (2.1) yields

$$\overset{*}{p}_{\frac{1}{2}} = \frac{v_m}{0.0618 \times 10^{-6} \, p_m} \left\{ \frac{4.50}{v_m} - \overset{*}{v}_{\frac{1}{2}} \right\} \tag{3.13}$$

The computer circuit for the pump end of the pipe is shown in fig.
3.5. In this circuit diagram the coefficients C_3 and C_4 are defined
as

$$C_3 = \frac{v_m}{0.0618 \times 10^{-6} \, p_m} \tag{3.14}$$

$$C_4 = \frac{4.50}{v_m} \tag{3.15}$$
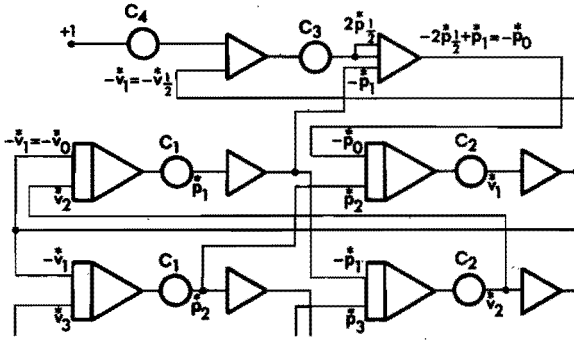
Fig.3.5. The analogue-computer circuit for the pump end of the pipe

3.2.1.3. The valve

The valve is the last element that is required to complete model A. As can be seen in fig. 3.6 we assume the valve to be at point $x = x_{n+\frac{1}{2}}$.
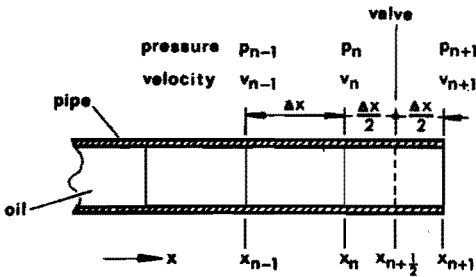
Fig.3.6. The valve end of the pipe

In the same way as we have done at the pump end of the pipe for $p_{\frac{1}{2}}$ and $v_{\frac{1}{2}}$, we now define

$$p_{n+\frac{1}{2}} = \frac{p_n + p_{n+1}}{2} \qquad (3.16)$$

$$v_n = v_{n+1} \qquad (3.17)$$

$$v_{n+\frac{1}{2}} = v_{n+1} \qquad (3.18)$$

30 For the analogue computations we take the valve discussed as example

in Sec. 2.3.4. The orifice area of this valve can be generally ex-
pressed as

$$A = A_0 + A_1 \cos \omega t + A_2 \cos 2\omega t \ldots + A_n \cos n\omega t \qquad (3.19)$$

where the coefficient A_0 still depends on the static pressure b_0.
The coefficients $A_2, \ldots\ldots\ldots, A_n$ are small and for the analogue com-
putations we will ignore them. The numerical values of A_0 for some
values of b_0 are given in table 3.1. The accessory values of b_1 from
fig. 2.9 and the numerical value of A_1 are also included in this
table.

b_0 10^5 N/m^2	b_1 10^5 N/m^2	A_0 10^{-6} m^2	A_1 10^{-6} m^2
25.00	5.75	4.2975	0.6225
35.00	9.50	3.4875	0.6225
45.00	13.60	2.9775	0.6225

Table 3.1. Numerical values of the orifice area
of the valve for some values of sta-
tic pressure b_0

With the aid of the Eqs. (2.4), (2.5) and (3.19) it is possible to
remodel Eq. (2.2) (see Sec. 2.3.3) as computer equation. Further,
using the cross-sectional area of the pipe (50.2×10^{-6} m^2), Eq.
(2.2) yields the following scaled equation

$$\overset{*}{p}_{n+\frac{1}{2}} = C_5 + \left\{ \frac{\overset{*}{v}_{n+\frac{1}{2}}}{(C_6 + C_7 \overset{*}{p}_{n+\frac{1}{2}})(C_8 + C_9 \cos C_{10}\tau)} \right\}^2 \qquad (3.20)$$

where

$$C_5 = \frac{3.5 \times 10^5}{2p_m} \qquad (3.21)$$

$$C_6 = 0.665 \qquad (3.22)$$

$$C_7 = 0.017 \times 10^{-6} \times p_m \qquad (3.23)$$

$$C_8 = \frac{A_0 \times 2^{\frac{1}{2}} \times p_m^{\frac{1}{2}}}{50.2 \times 10^{-6} \times \rho^{\frac{1}{2}} \times v_m} \qquad (3.24)$$

$$C_9 = \frac{A_1 \times 2^{\frac{1}{2}} \times p_m^{\frac{1}{2}}}{50.2 \times 10^{-6} \times \rho^{\frac{1}{2}} \times v_m} \qquad (3.25)$$

$$C_{10} = \frac{\omega}{\beta} \qquad (3.26)$$

Fig. 3.7 shows the computer circuit for the valve end of the pipe.
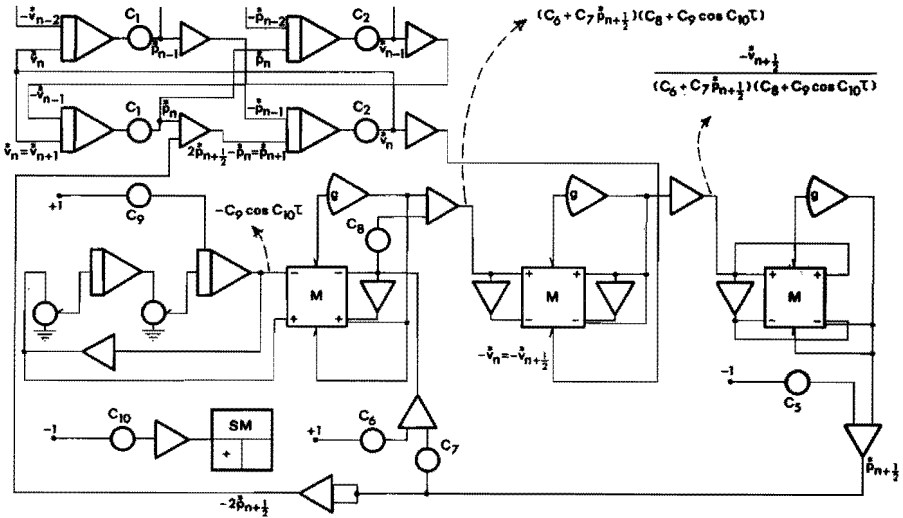
Fig.3.7. The analogue-computer circuit for the valve end of the pipe

3.2.2. The modulus of elasticity of the oil

With the aid of the elements discussed in Sec. 3.2.1 model A can be composed. Before starting the analogue computations, the parameters E, ρ, A_0, A_1, Δx, n, and ω have to be given a certain numerical value. However, the determination of the correct value of the modulus of elasticity of the oil forms a problem.

SCHLÖSSER (25) has shown that this modulus of elasticity depends not only on the pressure and the temperature of the oil, but also in a large measure on the air which is carried off by the oil. For example, if there is no air in the oil, the latter has a modulus of elasticity E = 16000 x 10^5 N/m^2 at a pressure of 35 x 10^5 N/m^2 and a temperature of 50 ^{o}C. However, this modulus of elasticity decreases to 8000 x 10^5 N/m^2 when the air content of the oil becomes 7.5%.

Furthermore, SCHLÖSSER has mentioned that the air content of the oil
32 in hydraulic systems is 6% on an average, while this percentage can

rise up to 18% in the case of a poorly designed system. VIERSMA (26)
has used for the modulus of elasticity of the oil the value
$E = 10000 \times 10^5$ N/m^2.

In connection with the foregoing it seems desirable to investigate
several values of the modulus of elasticity E. The numerical values
of the parameters E, ρ, A_0, A_1, Δx, n, and ω with which the analogue
study is started are mentioned in table 3.2 together with the scale
factors p_m, v_m, and β.

E	6000	10^5 N/m^2
E	8000	10^5 N/m^2
E	10000	10^5 N/m^2
ρ	856.2	kg/m^3
A_0	3.4875	10^{-6} m^2
A_1	0.6225	10^{-6} m^2
Δx	0.0997	m
n	11	--
ω	$0 \div 1000$	2π s^{-1}
p_m	100	10^5 N/m^2
v_m	20	m/s
β	1500	--

Table 3.2. Numerical values of parameters and scale
factors for model A

It is evident that n must be chosen as large as possible. Hence it
appears that Δx is as small as possible, if the pipe between pump
and valve has a fixed length. However, the choice of n is limited
by the total number of integrating amplifiers in the analogue com-
puter.

Now we can find the pressure as a function of time for every arbi-
trary frequency and at ten points on the pipe with the aid of the
analogue model A. An example about this is given in fig. 3.8, in
which the pressure p_9 has been written as a function of time t by
the analogue computer for a frequency of 100 Hz.
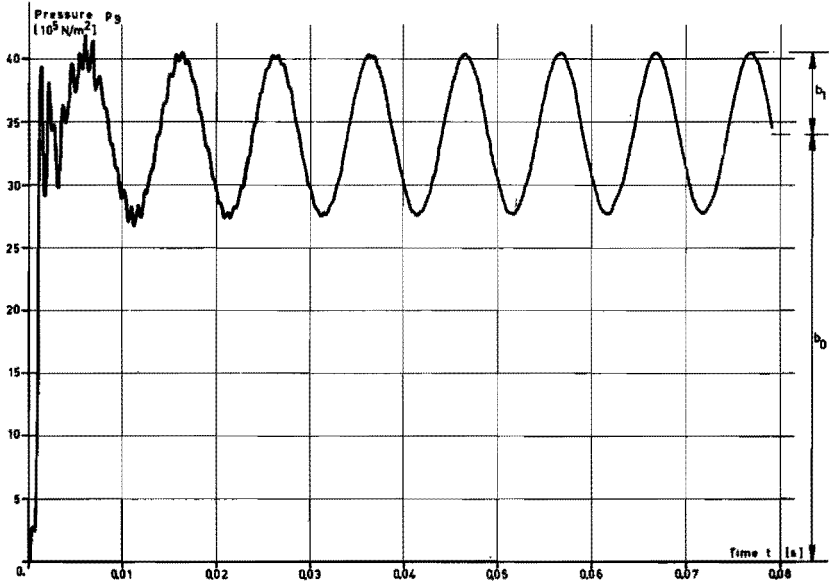
Fig.3.8. Example of an analogue solution; pressure p_9 as a function
of time t

In this example the modulus of elasticity E has the value
8000×10^5 N/m^2. We can see that after a relatively small number of
periods the solution only consists of a static part b_0 and a dynamic
part $b_1 \cos \omega t$. The values of b_0 and b_1 can be easily read from fig.
3.8. The value of b_0 practically agrees with the one mentioned in
table 3.1 for $A_0 = 3.4875 \times 10^{-6}$ m^2.

In order to obtain material which enables comparison with the analo-
gue solutions to be made, experiments were carried out in the labo-
ratory under the same conditions as for the analogue model. On the
34 pipe between pump and valve three measuring points were made, which

will further be denoted as MP 1, MP 2, and MP 3. The coordinates of
these points are given in table 3.3.

measuring point	coordinate x m
MP, 1	0.250
MP 2	0.574
MP 3	0.967

Table 3.3. Coordinates of the measuring points

At each measuring point the amplitude of the dynamic pressure can be
determined by means of a quartz pressure-transducer (Vibro-meter) and
a RMS-voltmeter (Hewlett-Packard). The static pressure b_0 has been
measured with the aid of an inductive pressure-transducer (Vibro-
meter).

The amplitude of the dynamic pressure consists not only of b_1, but
also of the several components of the noise of the pump (see Sec.
2.2). In order to determine the value of b_1 as accurately as possi-
ble, the valve was stopped after each experiment and then the sum of
all noise amplitudes was measured at the same value of b_0 which was
worked with during the experiment. The earlier measured signal of
the dynamic pressure can thus be corrected in order to get a better
approximation of the value of b_1.

In Sec. 3.2.1.3 it has already been reported that we use the same
valve as discussed in the example of Sec. 2.3.4. The value of A_1 for
this valve is mentioned in table 3.1. Still the piston of the valve
can be designed in several ways, as can be seen in fig. 2.5 (Sec.
2.3.1). However, during the experiments it turned out that it made
no difference as to the measured value of b_1 whether a frequency was
reached with a piston with two or with four waves.

The solutions of the analogue model under the conditions of table
3.2 are shown in fig. 3.9.

35
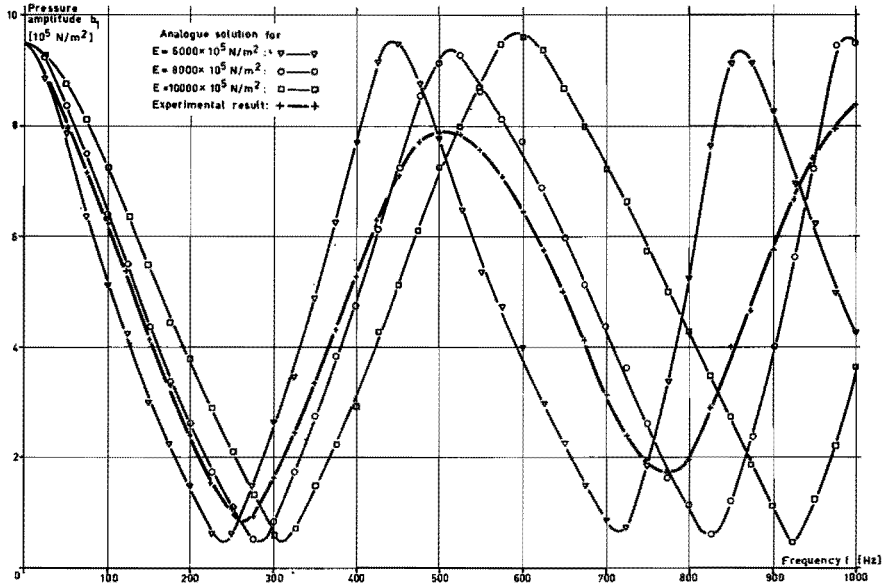
Fig.3.9. Pressure amplitude b_1 at MP 3 as a function of frequency f
for $b_0 = 35 \times 10^5$ N/m^2 and several values of E

Fig.3.10. Pressure amplitude b_1 at MP 3 as a function of frequency f
for $b_0 = 35 \times 10^5$ N/m^2 and E $= 8000 \times 10^5$ N/m^2

In this graph, which shows pressure amplitude b_1 at MP 3 as a function of frequency f, the experimental results are also shown. We can see that the analogue solution for $E = 8000 \times 10^5$ N/m^2 agrees best with the experimental result. The last-named graphs are once more shown in fig. 3.10.

3.2.3. The modulus of elasticity of the oil at seceral values of the static pressure b_0

All the investigations of the last section were made at a static pressure $b_0 = 35 \times 10^5$ N/m^2. As can be read in ref. (25), the modulus of elasticity would strongly depend upon the pressure exactly in the range in which we work (up to about 70×10^5 N/m^2). For this reason we carried out the investigations of the last section for other values of b_0.

Fig. 3.11 shows analogue solutions and experimental results at MP 3 for $b_0 = 25 \times 10^5$ N/m^2 ($A_0 = 4.2975 \times 10^{-6}$ m^2), as fig. 3.12 does for $b_0 = 45 \times 10^5$ N/m^2 ($A_0 = 2.9775 \times 10^{-6}$ m^2).
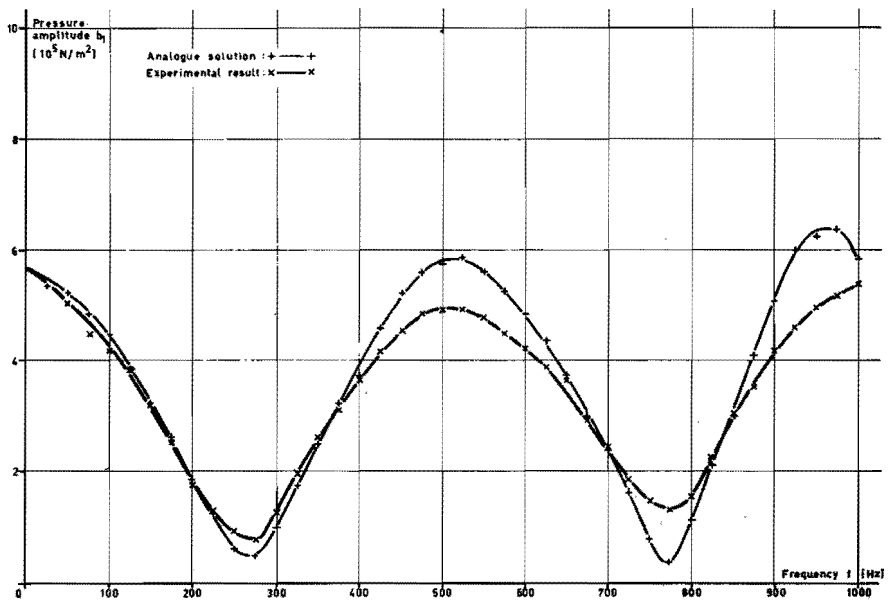
Fig.3.11. Pressure amplitude b_1 at MP 3 as a function of frequency f for $b_0 = 25 \times 10^5$ N/m^2 and $E = 8000 \times 10^5$ N/m^2

In both graphs the modulus of elasticity E in the analogue model has
the value 8000×10^5 N/m^2. For the rest the conditions are those of
table 3.2. From figs. 3.11 and 3.12 we can see that this value for E
also correspondends satisfactorily with the experimental results at
the static pressures referred to.

Fig.3.12. Pressure amplitude b_1 at MP 3 as a function of frequency f
for $b_0 = 45 \times 10^5$ N/m^2 and $E = 8000 \times 10^5$ N/m^2

3.2.4. Relation between b_1 and f at several points of the pipe

Besides at MP 3, measurements were carried out at MP 2 and MP 1. The
results are shown in figs. 3.13 and 3.14. As regards the analogue mo-
del, both graphs show the conditions of table 3.2 with
$E = 8000 \times 10^5$ N/m^2.
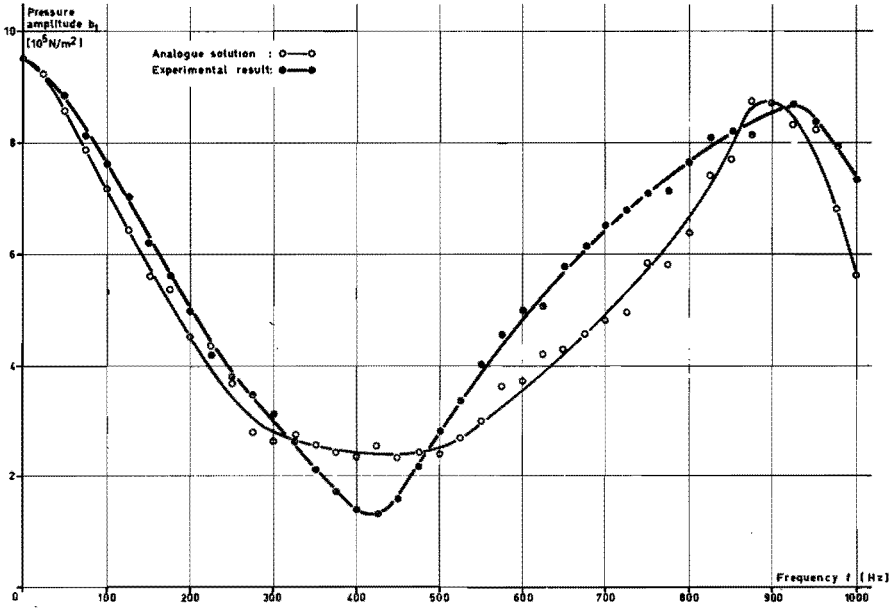
Fig.3.13. Pressure amplitude b_1 at MP 2 as a function of frequency f
for $b_0 = 35 \times 10^5$ N/m^2 and E = 8000 $\times 10^5$ N/m^2
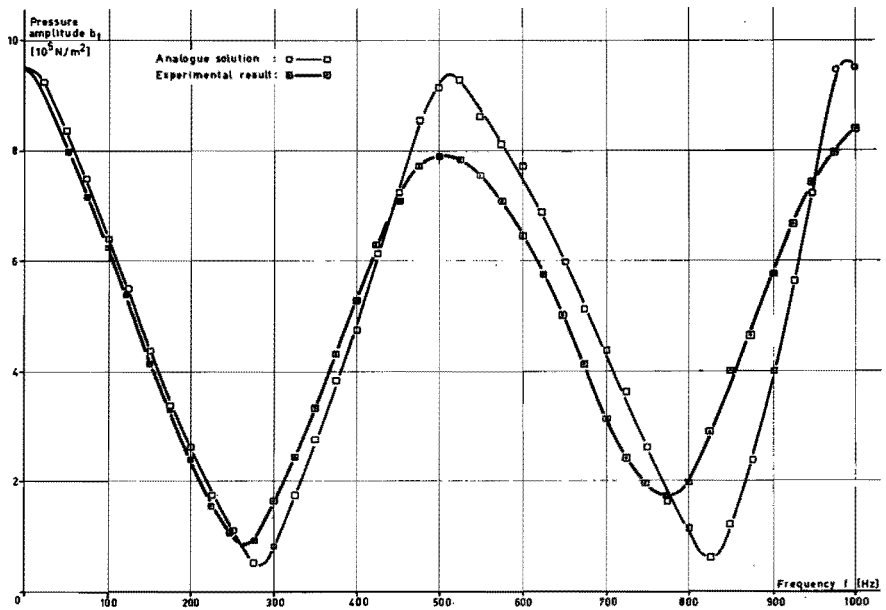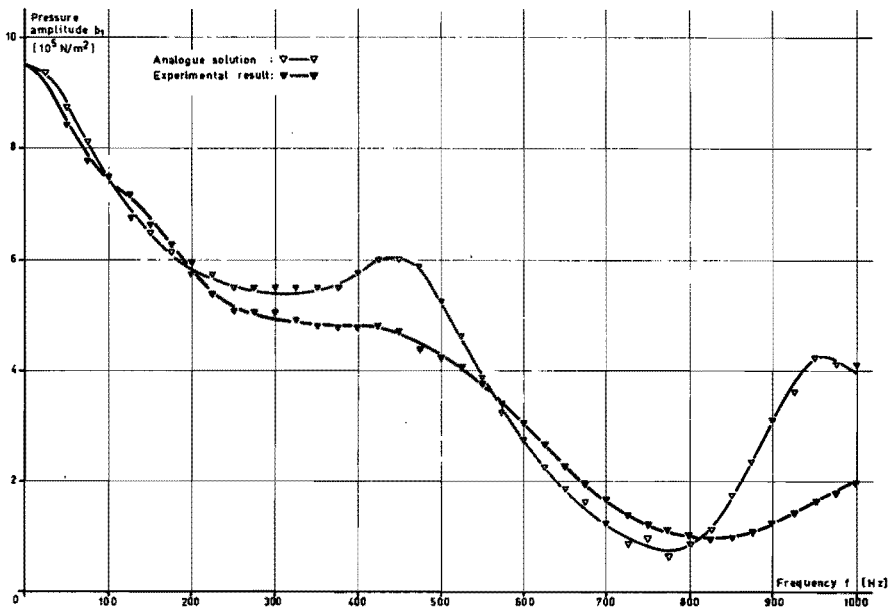

Fig.3.14. Pressure amplitude b_1 at MP 1 as a function of frequency f
for $b_0 = 35 \times 10^5$ N/m^2 and E = 8000 $\times 10^5$ N/m^2

The relations between b_1 and f at the several points are quite different from each other. We can see that according as we are nearing the pump, the derivative $\frac{db_1}{df}$ becomes generally smaller.

3.2.5. Discussion of the results of model A

From a qualitative comparison of the analogue and experimental results reasonable correspondence can be established. In general, we can say that the difference between analogue and experimental results is greater according as the frequency is higher. On the one hand this is probably due to the finite-difference approximation used for the derivatives with respect to x in the analogue model, on the other hand it seems likely that neglecting the damping in the analogue model has more influence at high frequencies than at low ones. A more quantitative impression of the differences mentioned is shown by table 3.4.

Fig.	average deviation
3.10	16.6%
3.11	12.3%
3.12	14.6%
3.13	13.8%
3.14	15.4%

Table 3.4. Average deviation of the experimental results with respect to the analogue solutions

This table gives for each diagram the average deviation of the experimental results with respect to the analogue solutions:

$$\frac{\displaystyle\int_{f = 0 \text{ Hz}}^{1000 \text{ Hz}} \left| b_1 \text{ anal.} - b_1 \text{ exp.} \right| df}{\displaystyle\int_{f = 0 \text{ Hz}}^{1000 \text{ Hz}} b_1 \text{ anal.} \, df} \times 100\%.$$

As can be seen in fig. 3.9 a change in the modulus of elasticity gives a multiplication of the graph of solution in the direction of the frequency axis. Now, if a solution has coordinates (f, b_1) in the graph with modulus of elasticity E_1, it obtains coordinates

$$\left\{ \left\{ \frac{E_2}{E_1} \right\}^{\frac{1}{2}} f, b_1 \right\}$$

when the modulus of elasticity changes into E_2. This can be easily derived from the Eqs. (3.1) and (3.2). By differentiating Eq. (3.1) with respect to t and Eq. (3.2) with respect to x, it is possible to transform these two equations into one second-order partial-differential equation with only p as dependent variable. Scaling the equation found for the analogue computer, we also find one quotient of parameters, which is comparable with the two quotients of parameters C_1 and C_2 of the Eqs. (3.8) and (3.9). The quotient of parameters of the second-order partial-differential equation contains among other factors the factor $\frac{E^{\frac{1}{2}}}{\beta}$, which causes the multiplication referred to. However, the second-order partial-differential equation is less suited to be solved on an analogue computer because differentiating the two wave equations results in the possibility of introduction of incorrect solutions.

If a small value of the derivative $\frac{db_1}{df}$ is required, the modulus of elasticity of the oil E has to be as large as possible. We have seen that in spite of precautions to keep air out of the oil (outlets of all pipes below oil surface, heating of the oil), the value of E for the present hydraulic plant may only be fixed at 8000×10^5 N/m^2 in the considered pressure range (see figs. 3.10, 3.11 and 3.12).

More interesting with respect to the relation between b_1 and f is the point on the pipe. The dependence between the last-named variables decreases strongly according as we approach the pump (see figs. 3.10, 3.13 and 3.14).

Up to now, we have ignored the length of the pipe. However, we can predict the influence of this parameter very easily with the Eqs. (3.6) and (3.7). In both equations the factor $\beta\Delta x$ appears in the same way. This means that a solution with coordinates (f, b_1) for a value Δx_1 obtains the coordinates $\left\{ \left\{ \frac{\Delta x_1}{\Delta x_2} \right\} f, b_1 \right\}$ for a value Δx_2. Fig. 3.15

gives an illustration of the last-named effect. In this diagram Δx is
varied, whereas n has been kept constant. For n and the remaining pa-
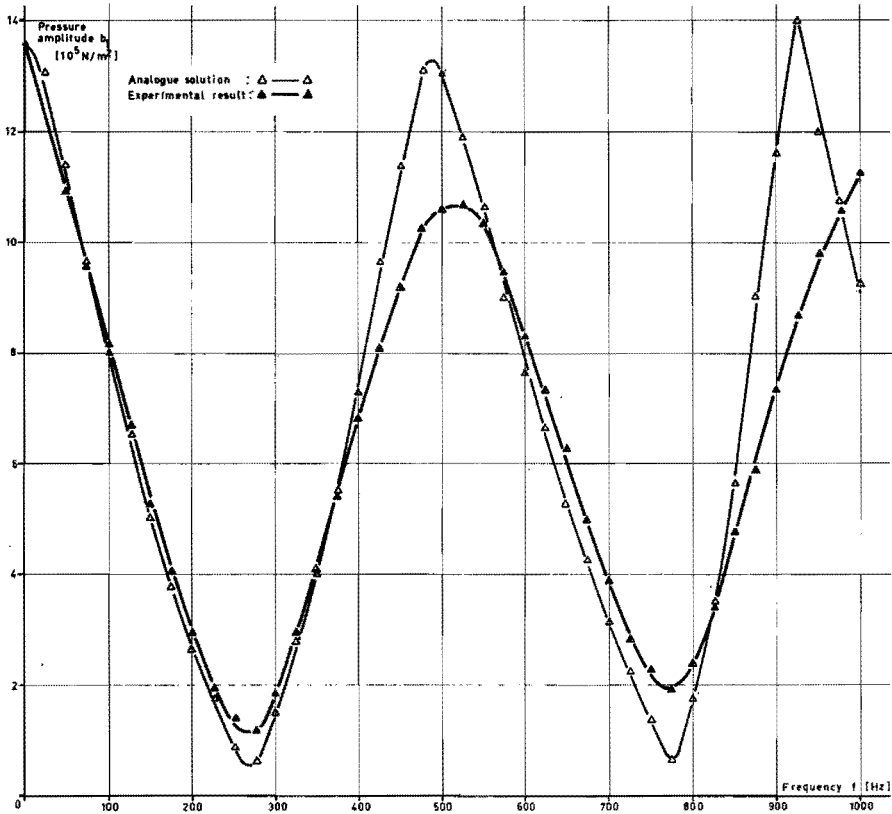rameters the values of table 3.2 with $E = 8000 \times 10^5$ N/m^2 are chosen
once more.
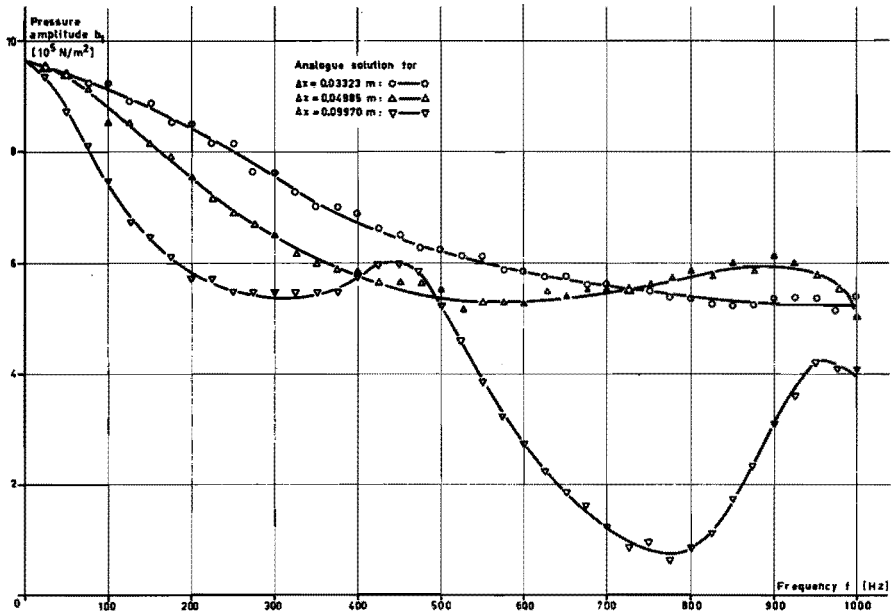
Fig.3.15. Pressure amplitude b_1 at MP 1 as a function of frequency f
for $b_0 = 35 \times 10^5$ N/m^2, $E = 8000 \times 10^5$ N/m^2 and several
values of Δx

Summarizing we may say that it is possible to give a rather good pic-
ture of the dynamic behaviour of model A with an analogue computer.
Once having established that the frequency should have only small in-
fluence on the pressure amplitude, we must take the length of the
pipe between pump and valve as short as possible and the pressure
wave has to be tapped close to the pump. Lastly, it is important to
keep air out of the oil.

3.3. Model B

3.3.1. The analogue elements of the model

42 In addition to the elements of model A discussed in Sec. 3.2.1, we

still need two new elements for the composition of model B, viz. a node of three pipes and a pipe end with exciter and machine tool (see fig. 3.1). These elements will be discussed in the following sections.

3.3.1.1. The node of three pipes

We consider the node as a place where three pipe ends come together (see fig. 3.16). The variables in these pipes are distinguished from each other by means of accent marks as shown in the latter figure.
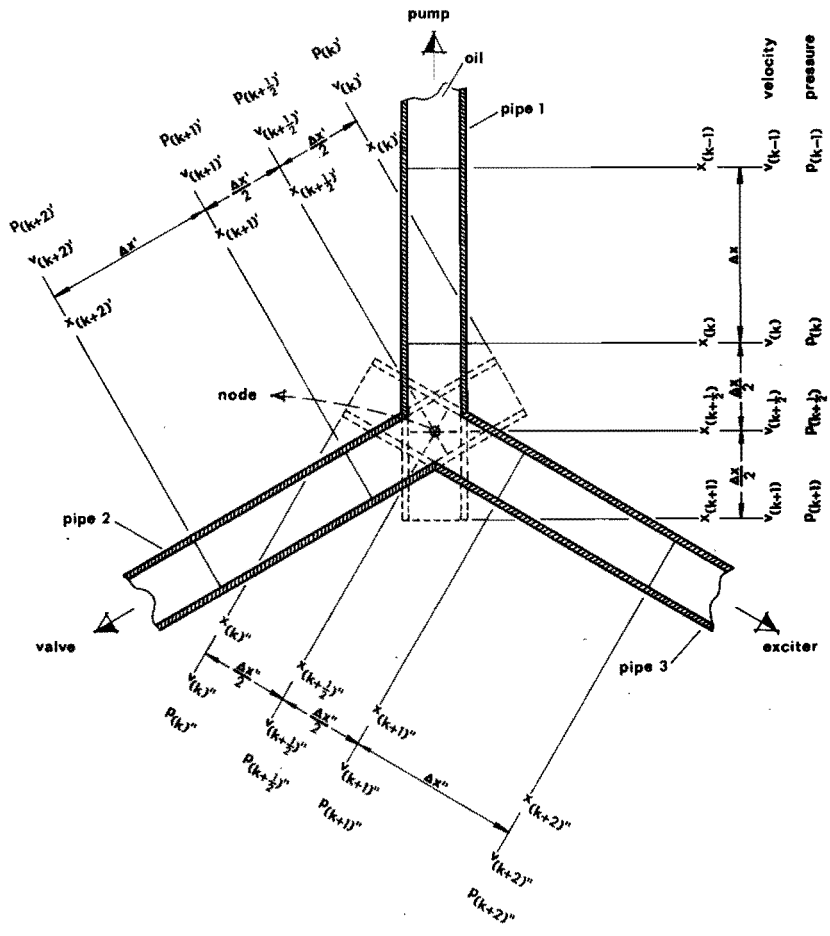
Fig.3.16. The node

For the analogue treatment of the node we use a similar method as the one applied in the Secs. 3.2.1.2 and 3.2.1.3 for the pump and valve end of the pipe in model A. As to the pressures, we define

$$P_{(k+\frac{1}{2})} = P_{(k+\frac{1}{2})'} \tag{3.27}$$

$$P_{(k+\frac{1}{2})} = P_{(k+\frac{1}{2})''} \tag{3.28}$$

$$P_{(k+\frac{1}{2})} = P_{(k)} \tag{3.29}$$

$$P_{(k+\frac{1}{2})} = P_{(k+1)} \tag{3.30}$$

$$P_{(k+\frac{1}{2})'} = \frac{P_{(k)'} + P_{(k+1)'}}{2} \tag{3.31}$$

$$P_{(k+\frac{1}{2})''} = \frac{P_{(k)''} + P_{(k+1)''}}{2} \tag{3.32}$$

The Eqs. (3.31) and (3.32) can be written as

$$P_{(k)'} = 2P_{(k+\frac{1}{2})'} - P_{(k+1)'} \tag{3.33}$$

and

$$P_{(k)''} = 2P_{(k+\frac{1}{2})''} - P_{(k+1)''} \tag{3.34}$$

respectively. As regards the velocities near the node, we define

$$v_{(k+\frac{1}{2})} = v_{(k+\frac{1}{2})'} + v_{(k+\frac{1}{2})''} \tag{3.35}$$

$$v_{(k+\frac{1}{2})} = \frac{v_{(k)} + v_{(k+1)}}{2} \tag{3.36}$$

$$v_{(k)'} = v_{(k+\frac{1}{2})'} \tag{3.37}$$

$$v_{(k)'} = v_{(k+1)'} \tag{3.38}$$

$$v_{(k)''} = v_{(k+\frac{1}{2})''} \tag{3.39}$$

$$v_{(k)''} = v_{(k+1)''} \tag{3.40}$$

With the aid of the Eqs. (3.35), (3.37) and (3.39), it is possible to rewrite Eq. (3.36) as

$$v_{(k+1)} = 2v_{(k)'} + 2v_{(k)''} - v_{(k)} \tag{3.41}$$

After scaling, we can use the Eqs. (3.27), ..., (3.30), (3.33), (3.34), (3.38), (3.40) and (3.41) in order to compose the circuit diagram for the node. This is shown in fig. 3.17.

Making use of $\Delta x'$ and $\Delta x''$ respectively, the coefficients $C_{1'}$ and $C_{1''}$ **44** are defined in the same way as the coefficient C_1 (see Eq. (3.8)).

pump
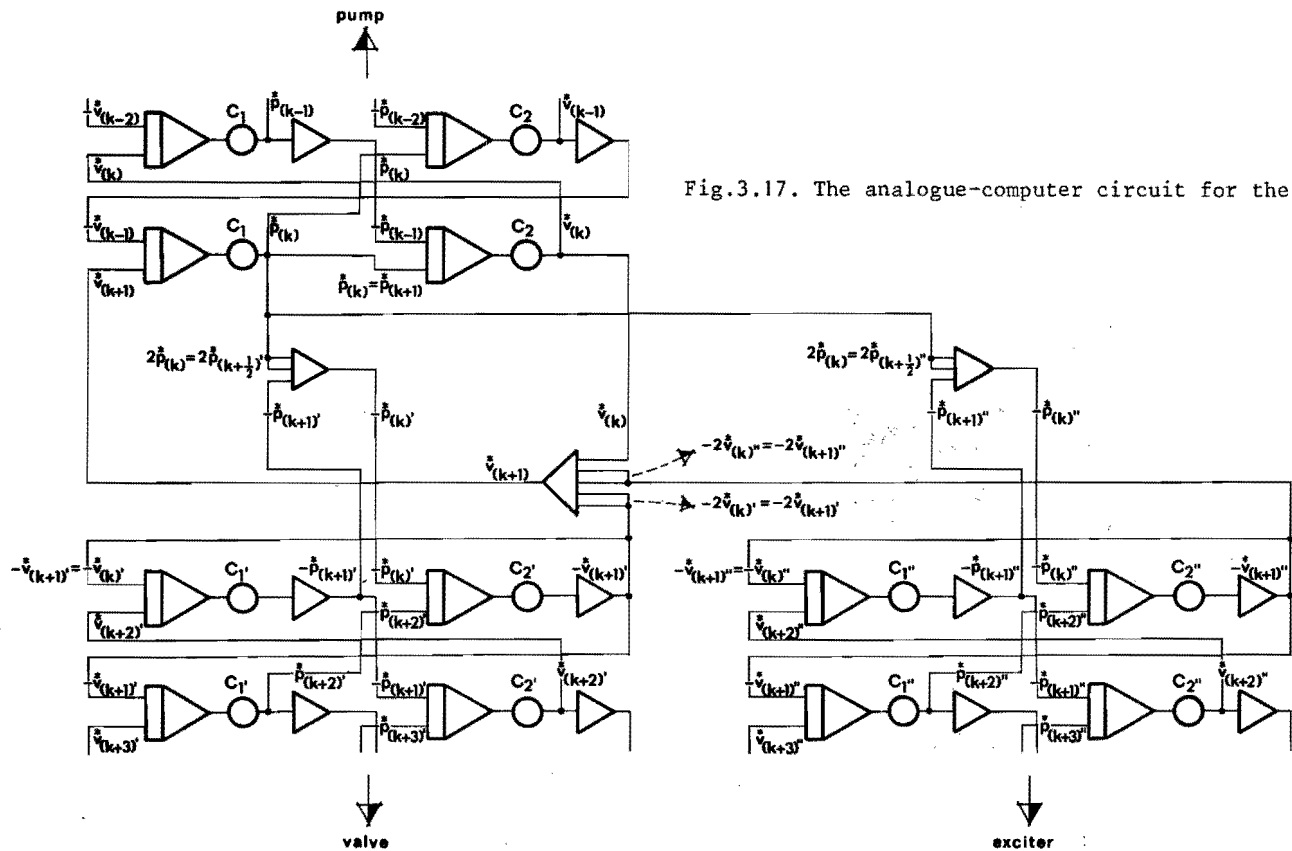
Fig.3.17. The analogue-computer circuit for the node

$\overset{*}{v}_{(k-2)}$ C_1 $\overset{*}{p}_{(k-1)}$ $\overset{*}{p}_{(k-2)}$ C_2 $\overset{*}{v}_{(k-1)}$

$\overset{*}{v}_{(k)}$ $\overset{*}{p}_{(k)}$

$\overset{*}{v}_{(k-1)}$ C_1 $\overset{*}{p}_{(k)}$ $\overset{*}{p}_{(k-1)}$ C_2 $\overset{*}{v}_{(k)}$

$\overset{*}{v}_{(k+1)}$ $\overset{*}{p}_{(k)}=\overset{*}{p}_{(k+1)}$

$2\overset{*}{p}_{(k)}=2\overset{*}{p}_{(k+\frac{1}{2})'}$ $2\overset{*}{p}_{(k)}=2\overset{*}{p}_{(k+\frac{1}{2})''}$

$\overset{*}{p}_{(k+1)'}$ $\overset{*}{p}_{(k)'}$ $\overset{*}{v}_{(k)}$ $\overset{*}{p}_{(k+1)''}$ $\overset{*}{p}_{(k)''}$

$\overset{*}{v}_{(k+1)}$ $-2\overset{*}{v}_{(k)}''=-2\overset{*}{v}_{(k+1)}''$

$-2\overset{*}{v}_{(k)}'=-2\overset{*}{v}_{(k+1)}'$

$-\overset{*}{v}_{(k+1)'}=\overset{*}{v}_{(k)'}$ C_1' $-\overset{*}{p}_{(k+1)'}$ $\overset{*}{p}_{(k)'}$ C_2' $-\overset{*}{v}_{(k+1)'}$ $-\overset{*}{v}_{(k+1)''}=\overset{*}{v}_{(k)''}$ C_1'' $-\overset{*}{p}_{(k+1)''}$ $\overset{*}{p}_{(k)''}$ C_2'' $-\overset{*}{v}_{(k+1)''}$

$\overset{*}{v}_{(k+2)'}$ $\overset{*}{p}_{(k+2)'}$ $\overset{*}{v}_{(k+2)''}$ $\overset{*}{p}_{(k+2)''}$

$\overset{*}{v}_{(k+1)'}$ C_1' $\overset{*}{p}_{(k+2)'}$ $\overset{*}{p}_{(k+1)'}$ C_2' $\overset{*}{v}_{(k+2)'}$ $\overset{*}{v}_{(k+1)''}$ C_1'' $\overset{*}{p}_{(k+2)''}$ $-\overset{*}{p}_{(k+1)''}$ C_2'' $\overset{*}{v}_{(k+2)''}$

$\overset{*}{v}_{(k+3)'}$ $\overset{*}{p}_{(k+3)'}$ $\overset{*}{v}_{(k+3)''}$ $\overset{*}{p}_{(k+3)''}$

valve   exciter

A similar remark can be held with respect to the coefficients $C_{2'}$ and $C_{2''}$ (see coefficient $\cdot C_2$ as defined in Eq. (3.9)).

3.3.1.2. The pipe end with exciter and machine tool

Fig. 3.18 shows this element in diagram. In this figure the machine
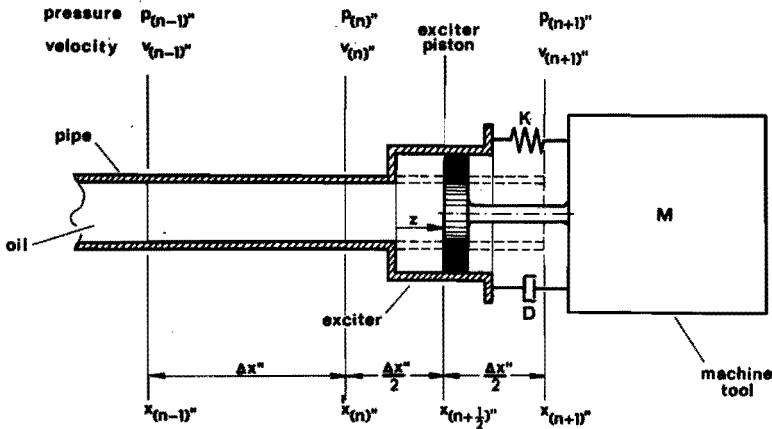
Fig.3.18. The pipe end with exciter and machine tool

tool is considered as a single-degree-of-freedom system, which is not
unusual in chatter research (see Sec. 1.1). We suppose that by the
static pressure of the oil the exciter piston is firmly connected
with the mass of the machine tool. The position of this mass can be
specified at any time by giving the coordinate z.
If the exciter piston is at point $x_{(n+\frac{1}{2})''}$, the vibration of the mass
can be described by Newton's law as

$$M \frac{d^2 z}{dt^2} = A_e \, P_{(n+\frac{1}{2})''} - D \frac{dz}{dt} - K z \qquad (3.42)$$

Furthermore, we assume

$$v_{(n+\frac{1}{2})''} = \frac{A_e}{A_p} \frac{dz}{dt} \qquad (3.43)$$

and

$$\frac{dz}{dt} = \dot{z} \qquad (3.44)$$

For the pipe end we can write

$$P_{(n)''} = P_{(n+1)''} \qquad (3.45)$$

$$P_{(n+\frac{1}{2})''} = P_{(n+1)''} \tag{3.46}$$

$$v_{(n+\frac{1}{2})''} = \frac{v_{(n)''} + v_{(n+1)''}}{2} \tag{3.47}$$

Substitution of Eq. (3.44) in Eq. (3.42) yields after scaling

$$\frac{d}{d\tau}(\overset{*}{z}) = C_{11}\ \overset{*}{P}_{(n+\frac{1}{2})''} - C_{12}\ \overset{*}{\dot{z}} - C_{13}\ \overset{*}{z} \tag{3.48}$$

where
$$C_{11} = \frac{A_e\ P_m}{M\ \beta\ \dot{z}_m} \tag{3.49}$$

$$C_{12} = \frac{D}{M\ \beta} \tag{3.50}$$

$$C_{13} = \frac{K\ z_m}{M\ \beta\ \dot{z}_m} \tag{3.51}$$

It can be easily verified that scaling of Eq. (3.44) yields

$$\frac{d}{d\tau}(\overset{*}{z}) = C_{14}\ \overset{*}{\dot{z}} \tag{3.52}$$

where
$$C_{14} = \frac{\dot{z}_m}{\beta z_m} \tag{3.53}$$

Finally, we can combine the Eqs. (3.43) and (3.44). After scaling, the result is

$$\overset{*}{v}_{(n+\frac{1}{2})''} = C_{15}\ \overset{*}{\dot{z}} \tag{3.54}$$

where
$$C_{15} = \frac{A_e\ \dot{z}_m}{A_p\ v_m} \tag{3.55}$$
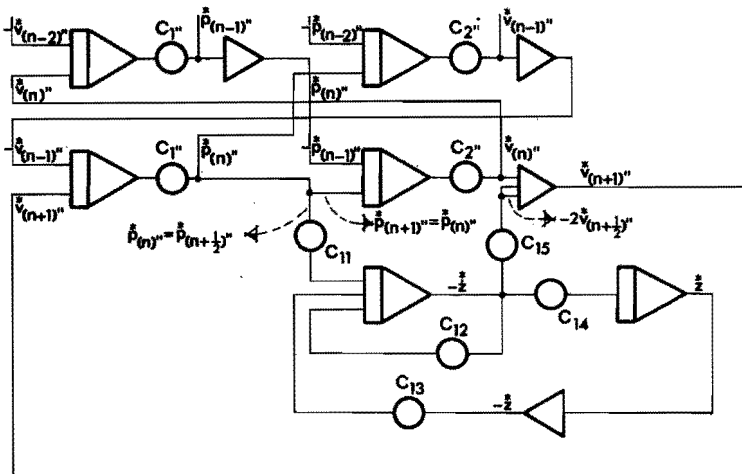

Fig.3.19. The analogue-computer circuit for the pipe end with exciter and machine tool

The Eqs. (3.48), (3.52) and (3.54) can be used to compose the compu-
ter diagram of the machine tool. After the Eqs. (3.45), (3.46) and
(3.47) are scaled, they form the link between the latter computer
diagram and that of the wave equations in the pipe. Thus we find the
computer diagram of fig. 3.19.

3.3.2. Results of model B

Investigation of model A resulted in a reasonable resemblance between
the analogue solutions and the experimental results (see Sec. 3.2.5).
Although two new analogue elements were needed for model B, they were
composed according to the same methods as those used for building the
elements of model A. For these reasons model B has only been investi-
gated on the analogue computer.

3.3.2.1. The influence of the pipe lengths l_1, l_2 and l_3 on b_1

The influence of these pipe lengths on the pressure amplitude b_1 ope-
rating on the exciter piston, was examined. In this section, the in-
fluence of the machine tool will be left out of consideration by vir-
tue of the supposition that in the computer diagram of fig. 3.19
$C_{11} = 0$.
Considering the results of model A, we take (l_1+l_2) as small as pos-
sible. However, for practical reasons this length cannot be taken
smaller than 0.25 m. At this fixed length of (l_1+l_2), several values
of the quotient $\frac{l_1}{l_2}$ are investigated. For l_3 values are chosen, which
may be required in the investigation of machine tools.

On account of the limited number of integrating amplifiers in the
PACE 231 R analogue computer, each pipe could only be divided into
five segments. This means that $n = 8$ and the node of the three pipes
is at point $x_{(4\frac{1}{2})}$ ($= x_{(4\frac{1}{2})'} = x_{(4\frac{1}{2})''}$). Now, variations in l_1, l_2 and
l_3 are applied in the computer diagram as variations in Δx, $\Delta x'$ and
$\Delta x''$ respectively.
In table 3.5 the numerical values of parameters and scale factors
are listed.

As can be seen in table 3.5 from the choice of A_0, all experiments
are carried out at a static pressure $b_0 = 35 \times 10^5$ N/m^2 (see also
table 3.1). Bearing in mind the results of model A, we take the mo-
dulus of elasticity of the oil E = 8000 $\times$ 10^5 N/m^2.

	E	8000	10^5 N/m^2
	ρ	856.2	kg/m^3
	A_0	3.4875	10^{-6} m^2
	A_1	0.6225	10^{-6} m^2
	$\Delta x + \Delta x'$	0.0625	m
$\dfrac{l_1}{l_2} = \dfrac{1}{2}$	Δx	0.0208	m
	$\Delta x'$	0.0417	m
$\dfrac{l_1}{l_2} = \dfrac{1}{1}$	Δx	0.0312	m
	$\Delta x'$	0.0312	m
$\dfrac{l_1}{l_2} = \dfrac{2}{1}$	Δx	0.0417	m
	$\Delta x'$	0.0208	m
$l_3 = 0.00$ m	$\Delta x''$	0.0000	m
$l_3 = 0.25$ m	$\Delta x''$	0.0625	m
$l_3 = 0.50$ m	$\Delta x''$	0.1250	m
$l_3 = 0.75$ m	$\Delta x''$	0.1875	m
	n	8	--
	ω	0 ÷ 1000	2π s^{-1}
	p_m	100	10^5 N/m^2
	v_m	20	m/s
	β	2000	--

Table 3.5. Numerical values of parameters and scale factors
for model B without a machine tool

If the experiments are carried out for $l_3 = 0.00$ m, we find the so-
lutions of fig. 3.20.
The solution for $\frac{l_1}{l_2} = \frac{1}{2}$ in this diagram can more or less be compared
with that for $\Delta x = 0.03323$ m in fig. 3.15.
Increase of l_3 gives solutions as shown in the figs. 3.21, 3.22 and
3.23.

Fig.3.20. Pressure amplitude b_1 on the exciter piston as a function of frequency f for $l_3 = 0.00$ m and several values of $\frac{l_1}{l_2}$

Fig.3.21. Pressure amplitude b_1 on the exciter piston as a function of frequency f for $l_3 = 0.25$ m and several values of $\frac{l_1}{l_2}$
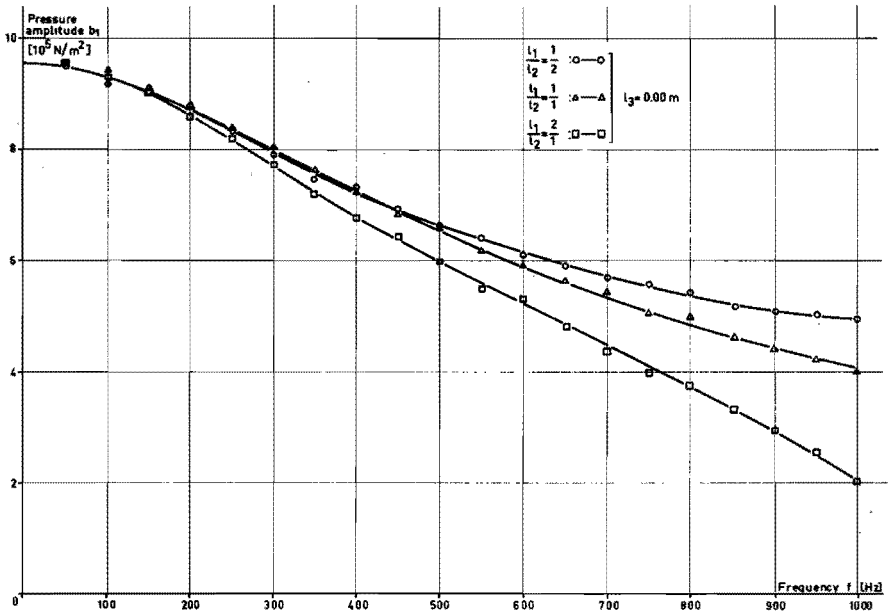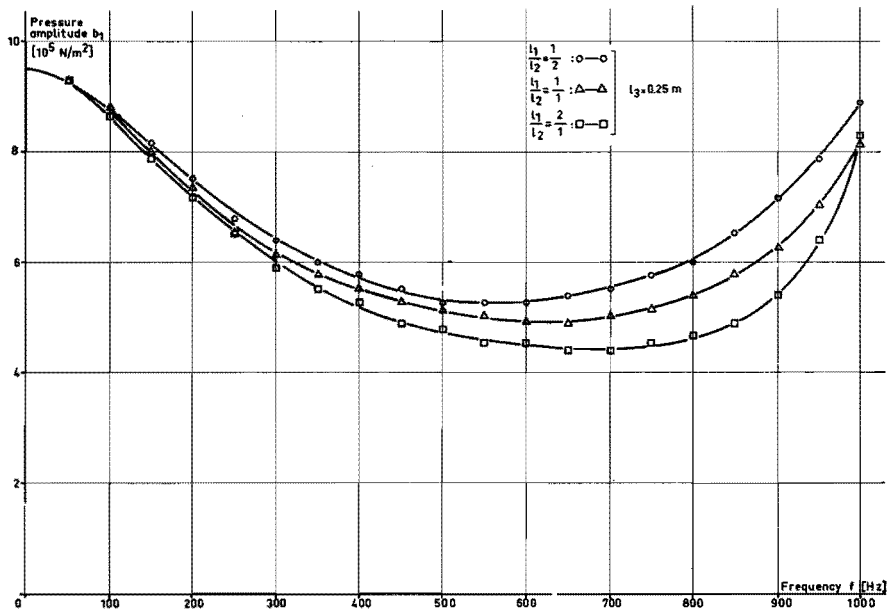
Fig.3.22. Pressure amplitude b_1 on the exciter piston as a function of frequency f for $l_3 = 0.50$ m and several values of $\dfrac{l_1}{l_2}$
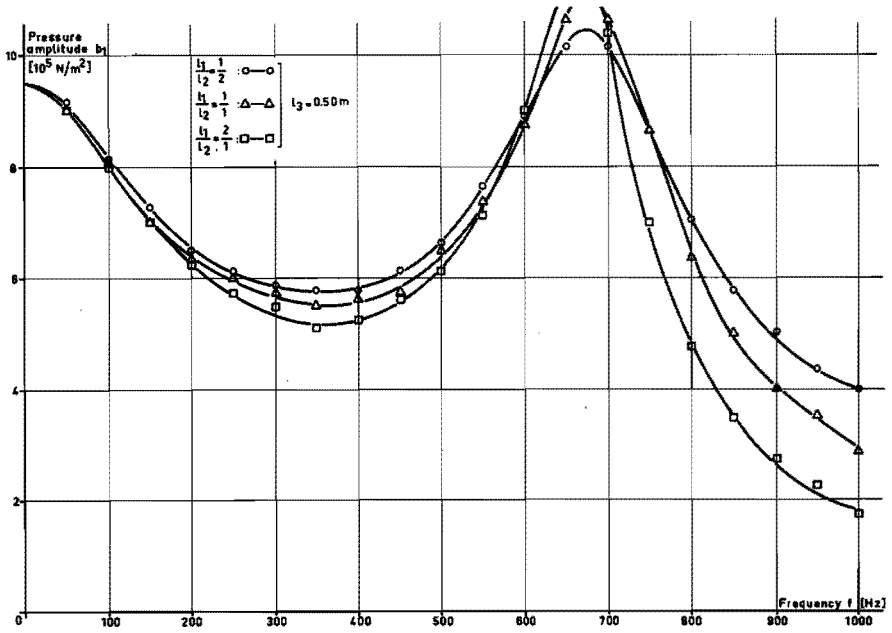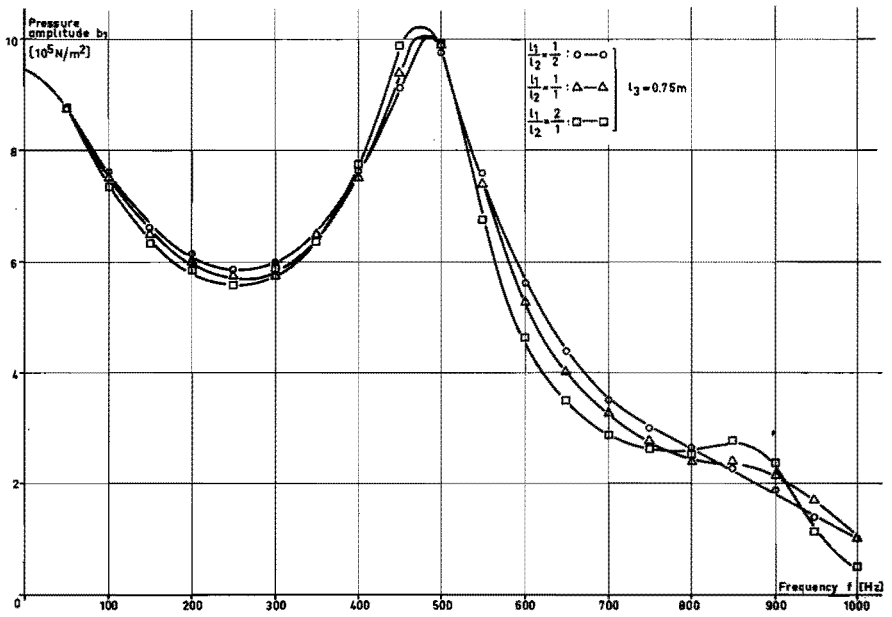

Fig.3.23. Pressure amplitude b_1 on the exciter piston as a function of frequency f for $l_3 = 0.75$ m and several values of $\dfrac{l_1}{l_2}$

3.3.2.2. The influence of the machine tool on $b_1.A_e$

The dynamic behaviour of the machine tool is determined by the varia-
bles M, D and K (see fig. 3.18). It is common practice to consider as
derived quantities

$$\omega_0 = \sqrt{\frac{K}{M}} \qquad\qquad (3.56)$$

and

$$q = \frac{\sqrt{M\,K}}{D} \qquad\qquad (3.57)$$

The quantity ω_0 is the angular velocity at the undamped natural fre-
quency of the single-degree-of-freedom system, while q is called the
amplification factor.

According to KOENIGSBERGER, PETERS and OPITZ (13), most of the natu-
ral frequencies of machine tools are in the range $0 \div 500$ Hz. So, in
this range, we take the natural frequencies of the machine tool of
model B.

The damping in machine tools is small. In this context, PETERS (27)
mentions that the amplification factor q of a conventional machine-
tool is always more than 17. Therefore, the machine tools in our
model study have amplification factors of 25, 50 and 75.

As may be expected, the values of the spring constant K are rather
high for machine tools. Even in the case of a less stiff machine-tool
as the radial drilling-machine, LANDBERG (28) mostly found spring con-
stants of about 1.5×10^7 N/m at a distance of 1 m from the column.
For our study we shall choose the order of magnitude of K in the
range $10^7 \div 10^8$ N/m.

It is customary to investigate the dynamic behaviour of a machine
tool by exciting the system with an alternating force the frequency
of which can be varied (see also Sec. 1.2). If we keep the amplitude
of this force constant, we find the maximum displacement-amplitude z_0
at natural frequency of the system. Apart from being related to M, D
and K, the amplitude z_0 depends upon the magnitude of the force am-
plitude. For practical reasons the frequency range to be investigated
is chosen in such a way that, besides the point with amplitude z_0, it
also contains the points with amplitude $\frac{z_0}{\sqrt{2}}$. In the case of a machine
tool such a range will seldom exceed 25 Hz.

52 Now, the analogue study of the complete model B is started with the

investigation of the influence of the movement of the exciter piston
on the force amplitude $b_1 . A_e$ operating on it. This is carried out for
a number of machine tools. Each machine tool is characterized by a
value of z_0 being the maximum displacement-amplitude of the system if
only the amplitude of the alternating force would be 100 N. The
values of ω_0 and q are kept unchanged for each machine tool. In table
3.6 the numerical values of parameters and scale factors for the in-
vestigated machine-tools are listed.

$z_0 = 20 \times 10^{-6}$ m	M	79.16	kg
$\omega_0 = 200 \times 2 \pi \, s^{-1}$	D	3.979	10^3 N.s/m
q = 25	K	12.50	10^7 N/m
$z_0 = 40 \times 10^{-6}$ m	M	39.58	kg
$\omega_0 = 200 \times 2 \pi \, s^{-1}$	D	1.989	10^3 N.s/m
q = 25	K	6.25	10^7 N/m
$z_0 = 80 \times 10^{-6}$ m	M	19.79	kg
$\omega_0 = 200 \times 2 \pi \, s^{-1}$	D	0.995	10^3 N.s/m
q = 25	K	3.12	10^7 N/m
$z_0 = 160 \times 10^{-6}$ m	M	9.90	kg
$\omega_0 = 200 \times 2 \pi \, s^{-1}$	D	0.497	10^3 N.s/m
q = 25	K	1.56	10^7 N/m
	z_m	0.5	10^{-3} m
	$\dot{z}_m$	0.25	m/s
	A_e	197.3	10^{-6} m^2
	A_p	50.2	10^{-6} m^2

Table 3.6. Numerical values of parameters and scale
factors for the machine tool of model B
(variation of z_0)

For the remaining parameters and scale factors of model B the values
of table 3.5 with $\frac{l_1}{l_2} = \frac{1}{2}$ and $l_3 = 0.25$ m are chosen, except for the   **53**

parameters A_0 and ω. For ω, values in a range near the natural fre-
quency of the machine tool are taken, while A_0 is chosen in such a
way that when the piston does not move ($z_0 = 0$ m), the magnitude of
the force amplitude $b_1.A_e$ on the piston is precisely 100 N in the
frequency range to be investigated. Now, this value of A_0 is further
used for exciting the machine tools of table 3.6. The results are
shown in fig. 3.24.

Fig.3.24. Force amplitude $b_1.A_e$ on the exciter piston as a function
of $\frac{\omega}{\omega_0}$ for $\omega_0 = 200 \times 2\pi$ s^{-1}, $q = 25$, $l_3 = 0.25$ m and se-
veral values of z_0

Next, the influence of ω_0 on the relationship between $b_1.A_e$ and $\frac{\omega}{\omega_0}$
is to be investigated at a constant product $z_0.\omega_0$. The numerical
values of the parameters of the investigated machine-tools are spe-
cified in table 3.7.

For the remaining parameters and scale factors we refer to table 3.5
$\left\{\frac{l_1}{l_2} = \frac{1}{2} \text{ and } l_3 = 0.25 \text{ m}\right\}$ and to table 3.6, except for A_0 and ω.
For the latter parameters the same remarks as made in the previous
investigation apply. The results of the investigation into the in-
54 fluence of ω_0 are given in fig. 3.25.

$z_0 = 160 \times 10^{-6}$ m	M	39.58	kg
$\omega_0 = 100 \times 2\pi$ s^{-1}	D	0.995	10^3 N.s/m
$q = 25$	K	1.56	10^7 N/m
$z_0 = 80 \times 10^{-6}$ m	M	19.79	kg
$\omega_0 = 200 \times 2\pi$ s^{-1}	D	0.995	10^3 N.s/m
$q = 25$	K	3.12	10^7 N/m
$z_0 = 40 \times 10^{-6}$ m	M	9.90	kg
$\omega_0 = 400 \times 2\pi$ s^{-1}	D	0.995	10^3 N.s/m
$q = 25$	K	6.25	10^7 N/m

Table 3.7. Numerical values of parameters for the
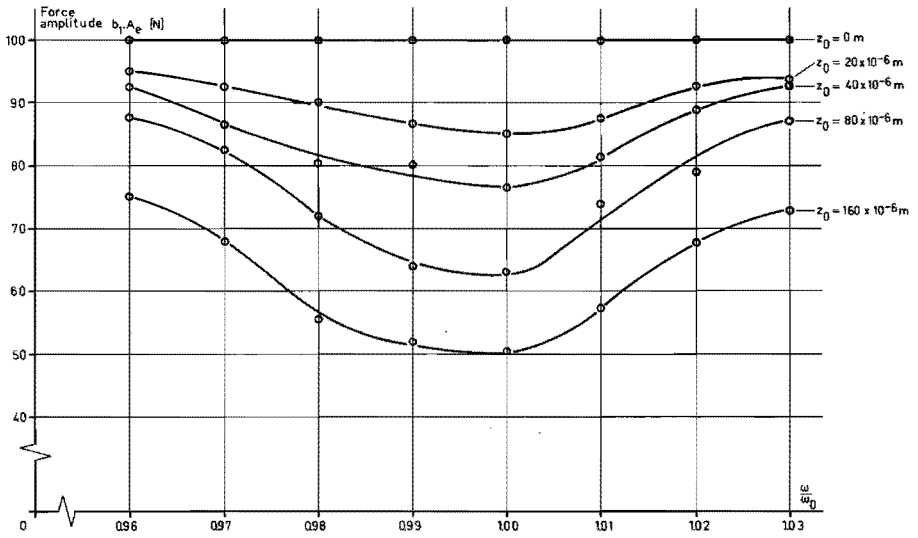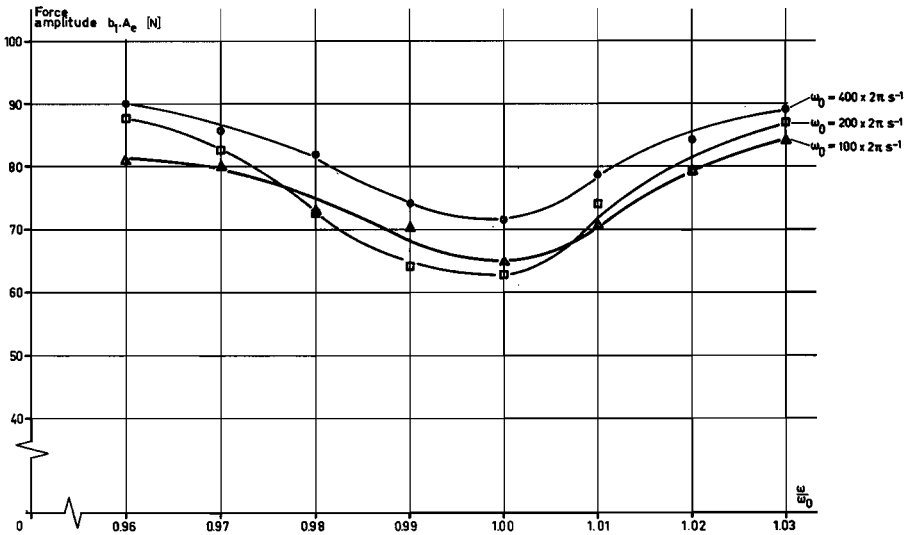machine tool of model B (variation of ω_0)

Fig. 3.25. Force amplitude $b_1 . A_e$ on the exciter piston as a function
of $\frac{\omega}{\omega_0}$ for $z_0 . \omega_0 = 16 \times 2\pi \times 10^{-3}$ m/s, $q = 25$, $l_3 = 0.25$ m
and several values of ω_0

Completely according to the same methods, the influence of q is de-
termined. For this purpose the numerical values of the parameters of **55**

the machine tools are specified in table 3.8, while the result is shown in fig. 3.26.

$z_0 = 80 \times 10^{-6}$ m	M	19.79	kg
$\omega_0 = 200 \times 2\pi$ s^{-1}	D	0.995	10^3 N.s/m
q = 25	K	3.12	10^7 N/m
$z_0 = 80 \times 10^{-6}$ m	M	39.58	kg
$\omega_0 = 200 \times 2\pi$ s^{-1}	D	0.995	10^3 N.s/m
q = 50	K	6.25	10^7 N/m
$z_0 = 80 \times 10^{-6}$ m	M	59.37	kg
$\omega_0 = 200 \times 2\pi$ s^{-1}	D	0.995	10^3 N.s/m
q = 75	K	9.38	10^7 N/m

Table 3.8. Numerical values of parameters for the machine machine tool of model B (variation of q)

Fig.3.26. Force amplitude $b_1.A_e$ on the exciter piston as a function of $\frac{\omega}{\omega_0}$ for $z_0 = 80 \times 10^{-6}$ m, $\omega_0 = 200 \times 2\pi$ s^{-1}, $l_3 = 0.25$ m and several values of q

Finally, the influence of the length l_3 on the relationship between $b_1 . A_e$ and $\frac{\omega}{\omega_0}$ has to be investigated for the machine tool figuring in table 3.6 as well as in the tables 3.7 and 3.8. Fig. 3.27 shows the result.
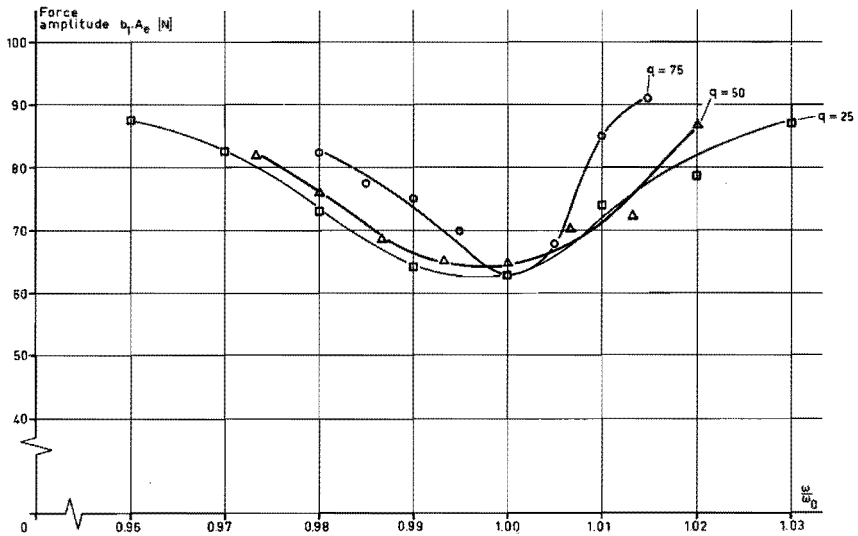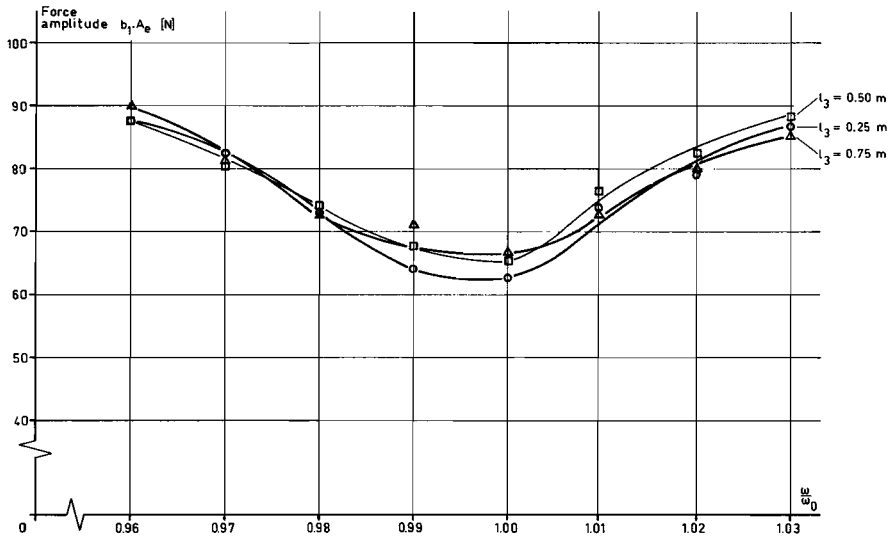

Fig.3.27. Force amplitude $b_1 . A_e$ on the exciter piston as a function of $\frac{\omega}{\omega_0}$ for $z_0 = 80 \times 10^{-6}$ m, $\omega_0 = 200 \times 2\pi$ s^{-1}, $q = 25$ and several values of l_3

3.3.3. Discussion of the results of model B

The investigation into the influence of the pipe lengths l_1, l_2 and l_3 on b_1 (see figs. 3.20, ..., 3.23) has shown that practically in the whole frequency range model B gives useful pressure amplitudes on the exciter piston. Roughly, the solution depends on the value of l_3. We can see that for $l_3 = 0.50$ m and $l_3 = 0.75$ m the higher frequencies are strongly damped. This gives us the possibility of decreasing the influence of the noise of the vane pump (see Sec. 2.2) on the exciter force, if at least the difference between the frequency of the dynamic pressure generated in the mechanically driven valve and the fundamental frequency of the noise (about 900 Hz) remains sufficiently large. In our experiments a minimum level of the noise was actually found in varying the length l_3.

At a fixed value of l_3 the solution for $\dfrac{l_1}{l_1 l_2} = \dfrac{1}{2}$ gives generally some smaller values of $\dfrac{db_1}{df}$. This value for $\dfrac{1}{l_2}$ has therefore been worked with in the investigation into the influence of the machine tool (Sec. 3.3.2.2). As already mentioned in the previous section, a range larger than 25 Hz will seldom be interesting for the detection of the resonance curve of a machine tool. Therefore, the proportional change of $\dfrac{db_1}{df}$ in such a range has been investigated for the figs. 3.20, ..., 3.23 $\left\{ \dfrac{l_1}{l_2} = \dfrac{1}{2} \right\}$. Fig. 3.28 shows the relationship between the proportional gradient of b_1 over 25 Hz $\left\{ \dfrac{db_1}{df} \times \dfrac{25}{b_1} \times 100\% \right\}$ and the frequency f.
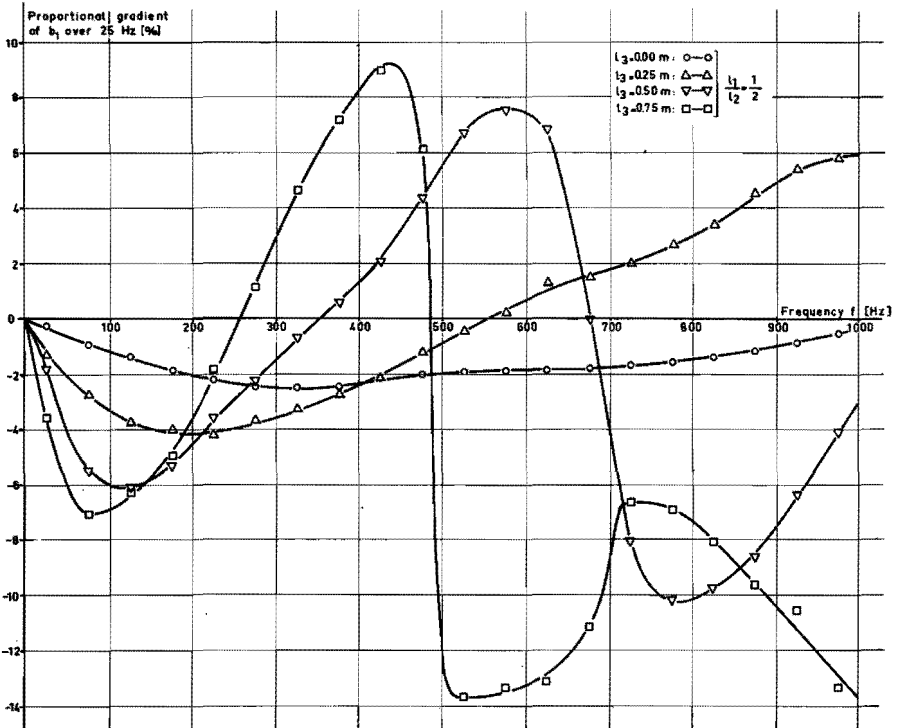

Fig.3.28. Proportional gradient of b_1 over 25 Hz as a function of frequency f for $\dfrac{l_1}{l_2} = \dfrac{1}{2}$ and several values of l_3

We can see that this percentage is generally small. This graph enables us to obtain the smallest gradient in a given case by taking the appropiate value of l_3.

The results of the investigation into the influence of the machine tool are shown in the figs. 3.24,....., 3.27. First of all, it has to be noticed that the accuracy, with which the points of these graphs are found, is considerably less than the accuracy of the foregoing analogue-solutions. This is due to the fact that the resonance curve of a machine tool is always situated in a rather narrow frequency range. We can see that variation of z_0 has by far the most influence. The force amplitude falls in the most unfavourable case $(z_0 = 160 \times 10^{-6}$ m) to half of its original value when the resonance of the machine tool is reached. Variation of the remaining parameters $(\omega_0$, q and l_3) has little influence.

Resuming, we can say that investigation of model B has proved that in the frequency range up to 1000 Hz useful force amplitudes on the exciter piston can be generated. Within the mentioned limits, pipe lengths cause seldom force-amplitude variations larger than 10% over a 25 Hz range. On the other hand, the machine tool can lead to force-amplitude variations of 50% over a same frequency range. It will be obvious that these force-amplitude variations are not allowed in the investigation of the dynamic behaviour of a machine tool. The next chapter explains in which way this amplitude can be kept constant.

4. A CONTROL SYSTEM FOR THE EXCITER FORCE

4.1. Introduction

The results obtained in the previous chapter with the analogue models
A and B (see Secs. 3.2.5 and 3.3.3) have been applied to the ultimate
design of the hydraulic plant as regards lengths of pipes and de-
aeration of the oil. However, we have seen that such measures are in-
sufficient to guarantee a reasonably constant dynamic-force during the
investigation of a machine tool. To this effect, a control system has
been designed. It is discussed in this chapter.

4.2. The control system

We have seen that in the high-pressure part of the hydraulic plant
discussed in Chap. 2 a static pressure b_0 and an alternating pressure
with amplitude b_1 act jointly. There is a relationship between b_0 and
b_1, which is given in fig. 2.9 for the valve discussed in Sec. 2.3.4.
Every point of this curve is related to a certain static orifice-area
A_{stat} of the mechanically driven valve. Hence, it is possible to
change the amplitude b_1 by variation of A_{stat}, which feature is used
in developing the control system. However, the variation of A_{stat} in
this system is not effected by a change in the axial position of the
piston of the mechanically driven valve (see fig. 2.4), but by means
of a pneumatically actuated control-valve (Conoflow) connected in pa-
rallel with the mechanically driven valve. Fig. 4.1.shows the control
system diagrammatically.

In this diagram, system 1 corresponds with the hydraulic plant dis-
cussed in Chap. 2, but for control valve 1. The high-pressure part of
this system is connected with the exciter (piston area A_e'). System 1
provides a static exciter-force of $b_0'.A_e'$ and a dynamic exciter-force
with an amplitude of $b_1'.A_e'$. System 2 is also connected with the ex-
citer (piston area A_e''). It actuates the exciter piston in a static
way only, which results in an exciter force of $b_0''.A_e''$.

60
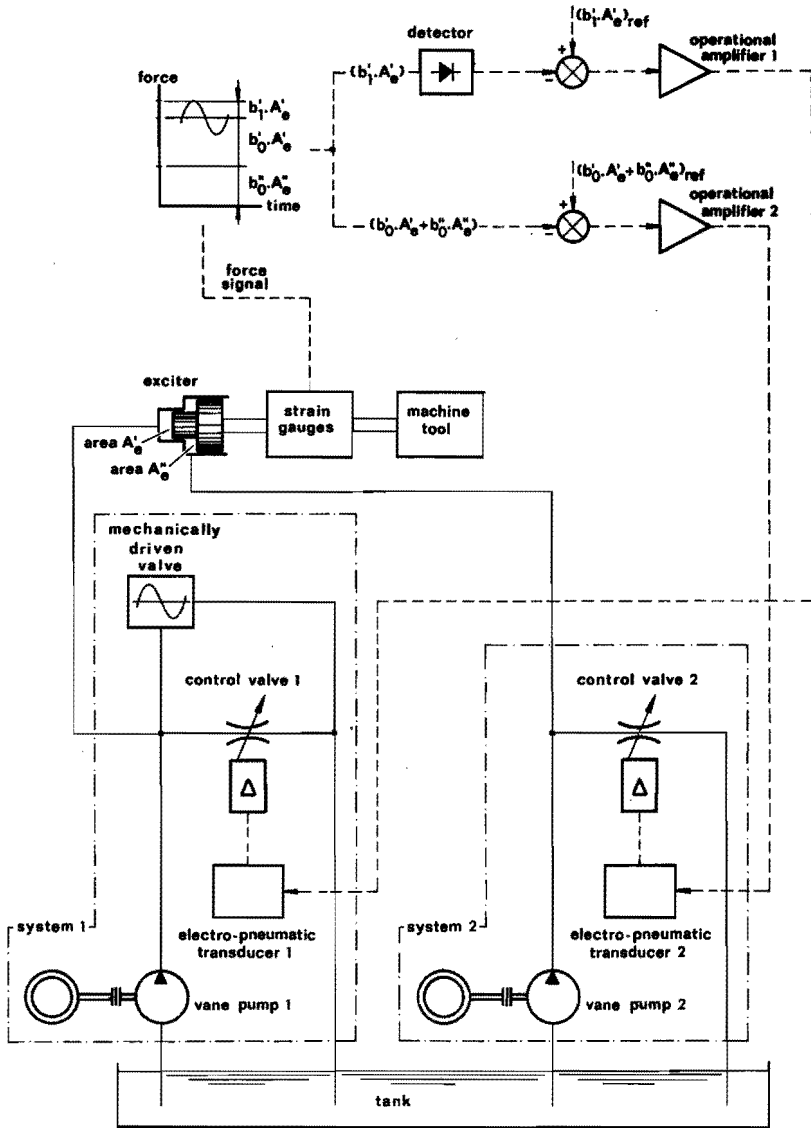
Fig.4.1. The control system

We assume that for a certain frequency the dynamic and the static force are equal to the reference values $(b_1'.A_e')_{ref}$ and $(b_0'.A_e' + b_0''.A_e'')_{ref}$ respectively. A change in the frequency of the dynamic force results in a variation of b_1' for reasons discussed in the previous chapter. In other words, a difference between $b_1'.A_e'$ and $(b_1'.A_e')_{ref}$ will occur. This difference, however, is reduced to zero

by the control action of operational amplifier 1 via electro-pneumatic transducer 1 and control valve 1. Another effect of this control action is a variation of b_0' and consequently of the static force $(b_0'.A_e' + b_0''.A_e'')$. This force is leveled by operational amplifier 2 to the pre-set value $(b_0'.A_e' + b_0''.A_e'')_{ref}$ via system 2.
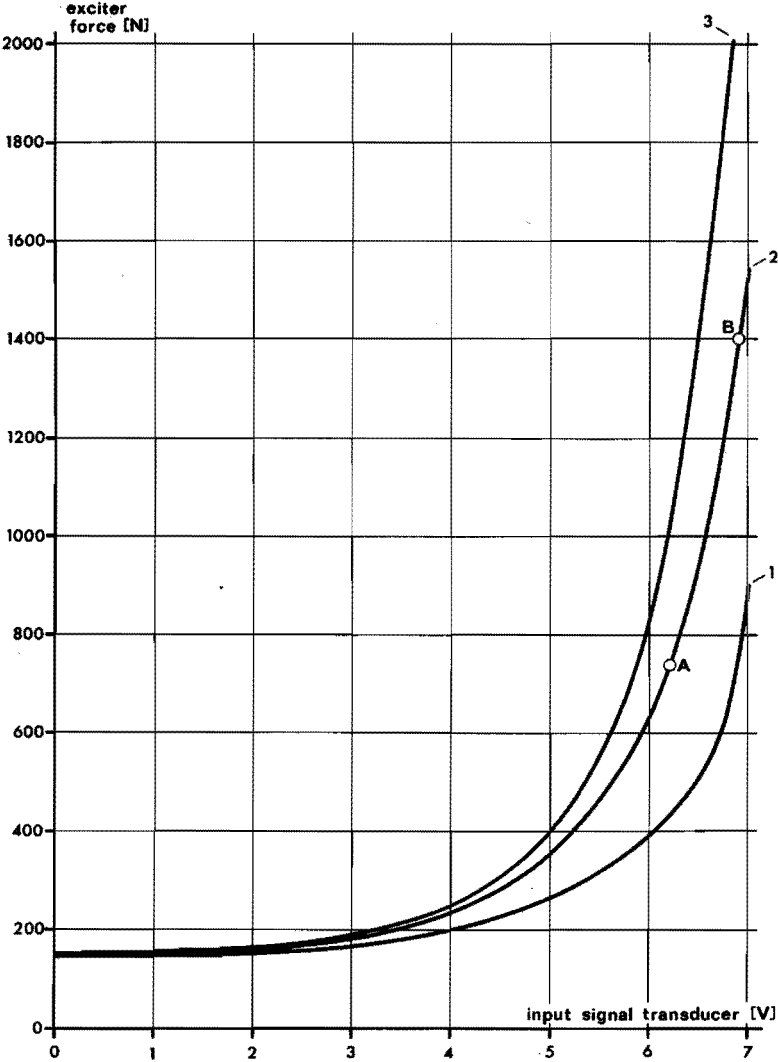
Fig.4.2. Static characteristics of control valve 1 for three axial positions of the piston of the mechanically driven valve

As already mentioned, the axial position of the piston of the mecha-
nically driven valve is not changed during control action. Evidently,
it is a parameter for each of the characteristics of fig. 4.2 of con-
trol valve 1.

In order to measure these characteristics, system 2 was put out of
operation. Curve 1 refers to a large orifice-area of the mechanically
driven valve, curve 3 to a small one. The control actions mainly oc-
cur in the range from 5 to 7 V input voltage of the transducer. From
the graph it will be seen that the portion AB of curve 2 may be con-
sidered to be a straight line. The gradient of this line (943 N/V) is
the value of the transfer function of system 1 in this part of curve
2 for a frequency f = 0 Hz. However, when we pass through AB dynami-
cally, the transfer-function mentioned is a complex quantity which
depends upon the frequency of the input signal. Fig. 4.3 shows the

Fig.4.3. Bode-diagram of the transfer function of system 1   **63**

Bode-diagram of the transfer function of system 1 for the length AB
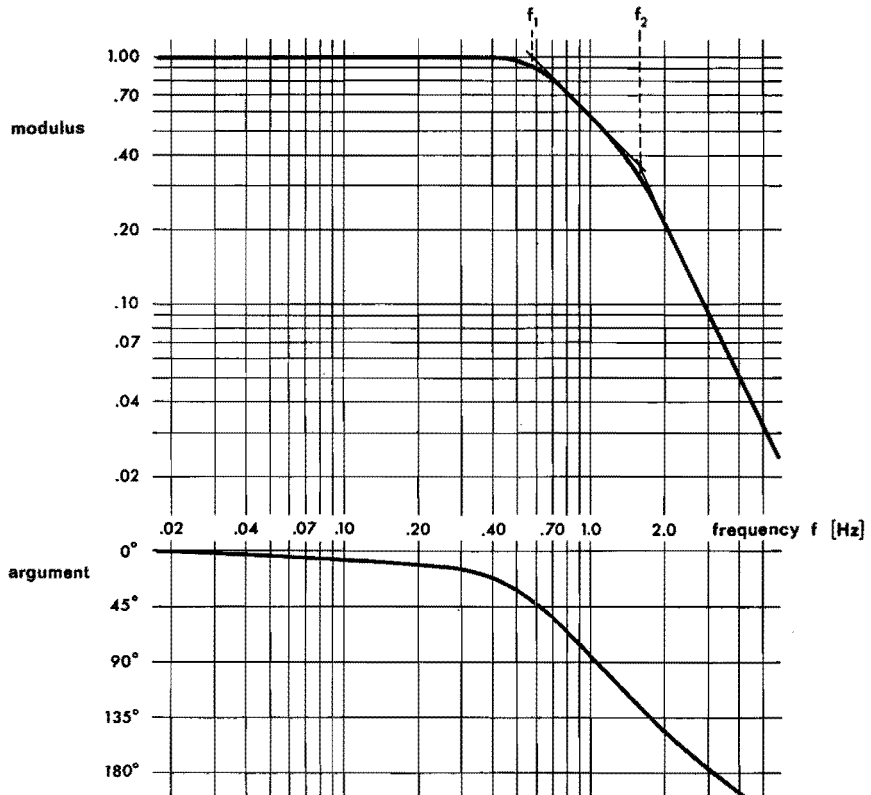of curve 2. In this figure the value of the transfer function for a
frequency f = 0 Hz has been assumed to be equal to 1.

In the experiments necessary to obtain this Bode-diagram, the length
of the pipe to the exciter (l_3) has been taken 0.75 m. We can see
that up to a frequency f_1 = 0.57 Hz the transfer function of system 1
has a value which is practically equal to the static one. For a fre-
quency f_2 = 1.60 Hz the argument of the transfer function is about
135°. The corresponding value of the modulus is 0.36. This value has
been used, together with similar values out of other working-areas of
fig. 4.2, to design operational amplifier 1.
System 2 has been investigated in the same way.

4.3. Accuracy of the control system.

Naturally, the accuracies with which the static and the dynamic force
are kept constant by the control system depend upon the adjustment of
the electronic equipment of the system. If the adjustment is correct,
the standard deviations are small percentages of the quantities con-
trolled.

The results of longitudinal excitation of an experimental drilling-
machine (Hettner) which will also come up for discussion in Chap. 5,
may serve as an example. Table 4.1 shows four series of measuring
points. The exciter was placed between drill (in dynamometer) and table.

series	number of measuring points	static force		dynamic force	
		N	standard deviation %	N	standard deviation %
1	9	785	5.1	39.8	0.8
2	6	740	3.5	39.7	0.0
3	7	737	4.3	40.0	0.4
4	9	707	3.9	40.3	0.2

Table 4.1. Accuracies of the control system

The measuring points are always chosen in a range around a certain
natural frequency (about 390 Hz) of the drilling machine. The maximum
64 displacement-amplitude measured between table and drill was about 2 μm.

5. THE NYQUIST-DIAGRAM OF A MACHINE TOOL

5.1. Introduction

In Sec. 1.2 we already remarked that the response of a machine tool
that has been excited can be recorded in two different ways. So we
find that LEMON and LONG (10) make use of Bode-diagrams, whereas
PETERS and VANHERCK (7) and REHLING (14) always give the transfer
function of a machine tool in the form of a Nyquist-diagram. We have
chosen the latter diagram, because we will use the method of PETERS
and VANHERCK (see Secs. 1.1 and 1.2) for chatter research.

If the machine tool is excited by a force F_1 cos ωt, a displacement
y_1 cos ($\omega t - \phi$) will generally be the result. The magnitudes can be
plotted in a polar diagram (Nyquist-diagram) as can be seen in fig.
5.1.

Fig.5.1. Nyquist-diagram
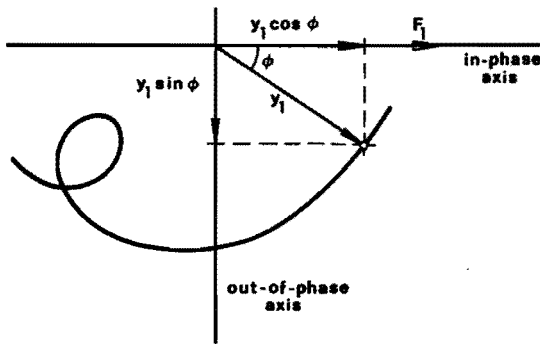
In this diagram the force vector coincides with the horizontal axis.
Decomposing of y_1 results in a component y_1 cos ϕ in phase with F_1
and a component y_1 sin ϕ which is $\pi/2$ rad out of phase with F_1. The
two components are the coordinates of one point of the Nyquist-curve.
We obtain other points of this curve by varying the frequency of the
dynamic force.

The general procedure for realising Nyquist-curves of mechanical vi-
bratory systems, which has been described by VON BASEL and VAN ZANTEN
(29), starts from two harmonic signals (B_1 cos ωt and B_1 sin ωt),
the frequency of which is the same as that of the force signal
F_1 cos ωt. We notice that B_1 cos ωt and F_1 cos ωt are in phase, whi-
le B_1 sin ωt and F_1 cos ωt are π/2 rad out of phase. If we multiply
the displacement signal by B_1 cos ωt and B_1 sin ωt respectively, we
find as average values

$$\frac{1}{2\pi} \int_{\omega t = 0}^{2\pi} y_1 \cos (\omega t - \phi) \, B_1 \cos \omega t \, d(\omega t) = \frac{B_1}{2} y_1 \cos \phi$$

and
$$(5.1)$$

$$\frac{1}{2\pi} \int_{\omega t = 0}^{2\pi} y_1 \cos (\omega t - \phi) \, B_1 \sin \omega t \, d(\omega t) = \frac{B_1}{2} y_1 \sin \phi$$

$$(5.2)$$

Apart from the scale factor $\frac{B_1}{2}$, the results of the Eqs. (5.1) and
(5.2) are the coordinates of the vector y_1 in the Nyquist-curve of
fig. 5.1. Now, if we can work out these average products, we can
record the Nyquist-diagram with the aid of an XY-recorder. A merit
of the method described is its frequency selectivity (wattmetric
principle). This method can be realised in several ways.
First, there is the multiplication necessary in the Eqs. (5.1) and
(5.2). For this multiplication VON BASEL and VAN ZANTEN (29) used
the quarter-square method. Logarithmic adding is also a possibility
and this is used by LEMON and LONG (10) in their equipment for plot-
ting Bode-diagrams. We, however, use Hall-probes for the multiplica-
tion.
Next, we can generate B_1 cos ωt and B_1 sin ωt in several ways.
Starting from the force signal and introducing a phase rotation of
π/2 rad with a Dome-filter is one possibility. VON BASEL and VAN
ZANTEN derive the cosine and sine signal directly from a two-phase
generator which also drives the electro-dynamic exciter. We on our
part generate B_1 cos ωt and B_1 sin ωt by means of the rotating pis-
ton of the mechanically driven valve (see Sec. 2.3).
The present chapter will give a description of our equipment for
recording Nyquist-diagrams. Some results obtained during the inves-
tigation of an experimental drilling machine will conclude the
66 chapter.

5.2. Equipment

5.2.1. General description

In order to make the mechanically driven valve also suitable for the purpose described in the previous section, an extension of the construction discussed in Sec. 2.3.1 was necessary. Fig. 5.2 shows this extension.
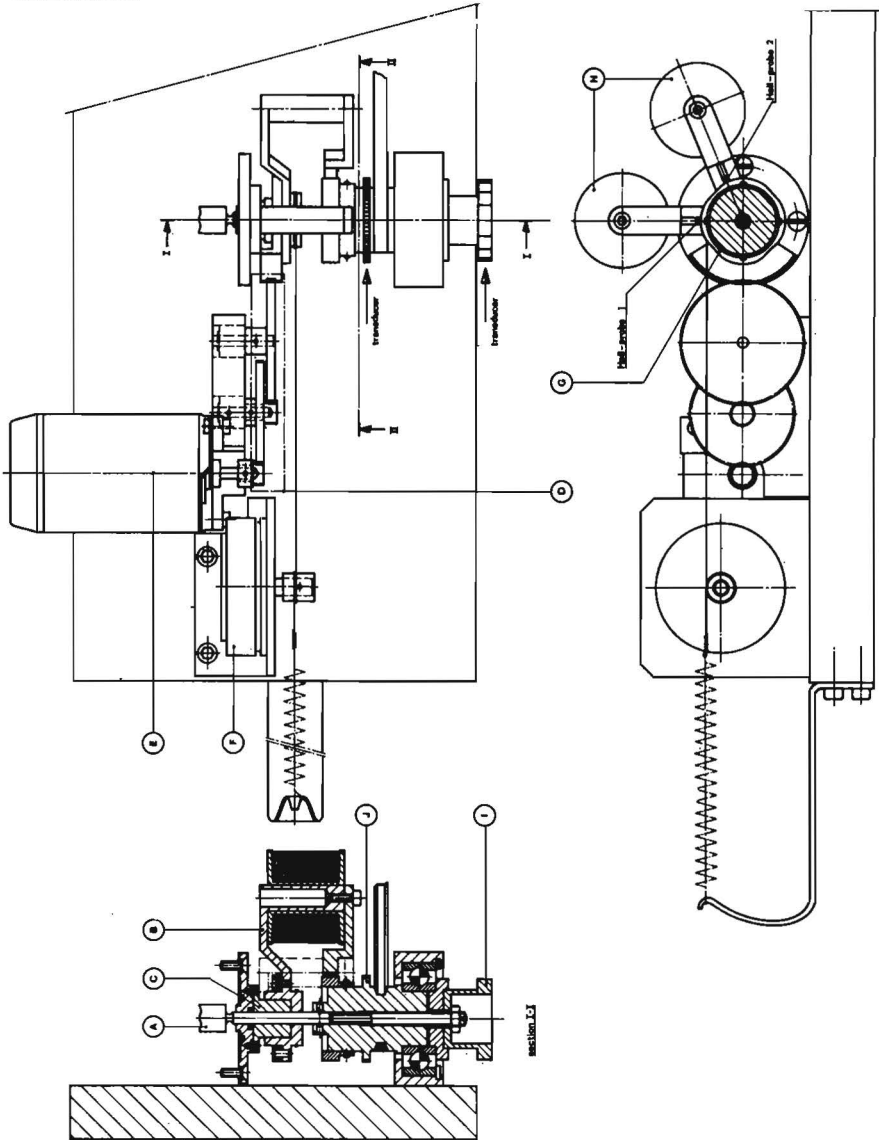

Fig.5.2. Extension of the mechanically driven valve

In this figure, we can distinguish the rotary piston A.
The fork B, which can rotate on the bronze cylinder C, is the most
important extension. The position of this fork can be changed with
the aid of the toothed wheels D by the stepping motor E. Potentiome-
ter F indicates the position of the fork. The Hall-probes 1 and 2
are glued on to the ends of the arms of the fork. The rotary piston
is driven by a V-belt in the way discussed in detail in Sec. 2.3.2.
The width of the air gaps between the Hall-probes and the sine-wheel
G depends upon the angular position and the shape of this wheel. Ex-
citation of the coils H results in a magnetic field in the air gaps
perpendicular to the surface of the Hall-probes. In addition to the
number of ampere turns of the coil, the magnetic induction depends
upon the width of the air gap.
The sine-wheel is firmly connected to the rotary piston and, conse-
quently, has the same speed of rotation as the piston. The sine-wheel
and the fork have been made so that the magnetic induction in the
air gap corresponding with Hall-probe 1 varies with $B_1 \cos \omega t$, while
the magnetic induction in the other air gap varies with $B_1 \sin \omega t$.
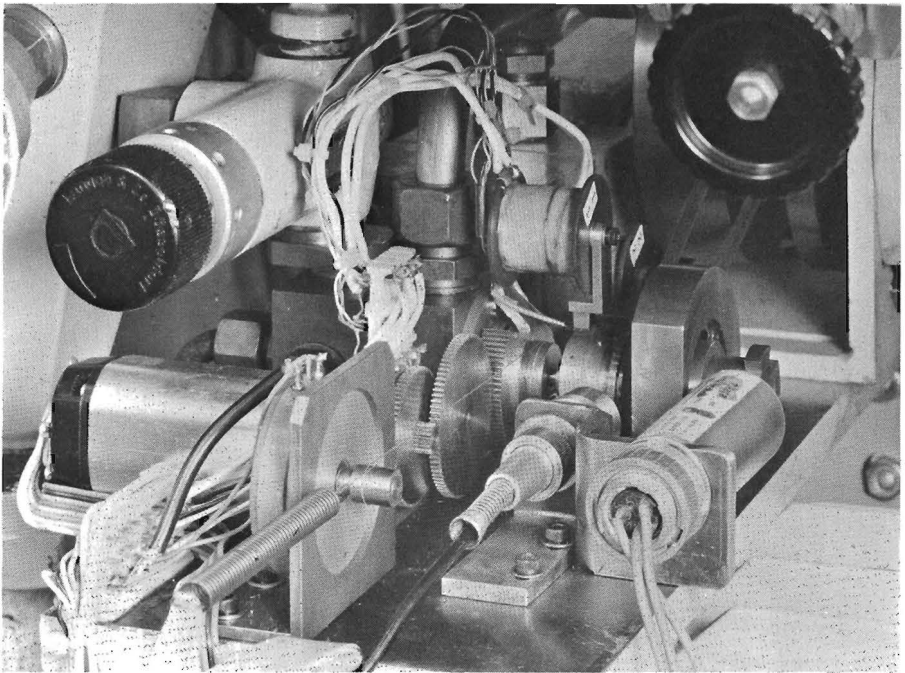
Fig.5.3. Photograph of the extension unit

Of course, the magnetic inductions in the air gaps have a constant component (B_0).

Lastly, the device has two toothed wheels I and J for frequency measurements. Fig. 5.3 shows a photograph of the extension unit discussed.

5.2.2. The Hall-effect

The Hall-effect is a phenomenon that was discovered in 1879. However, it was so small that it remained little more than a laboratory curiosity for many years. Around 1955 semi-conducting materials became available that resulted in technical applications of the effect. It will be described with the help of fig. 5.4.
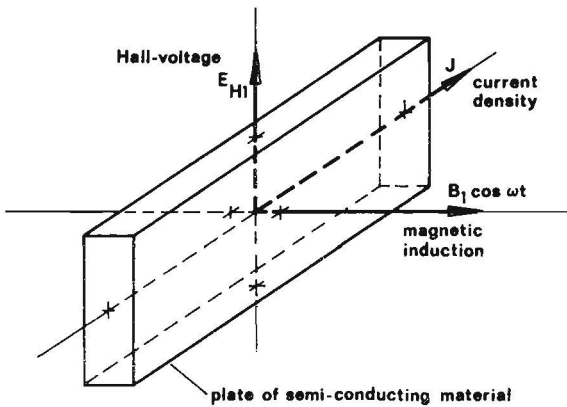
Fig.5.4. The Hall-effect

A plate of semi-conducting material is placed in a magnetic field. In fig. 5.4, the induction of this field is assumed to be B_1 cos ωt (see Sec. 5.2.1, Hall-probe 1). Furthermore, through the plate flows a current (current-density vector J). Now, the Hall-effect finds expression as a voltage E_{H1} which is produced across the conductor perpendicular to the plane through the direction of the current and the magnetic field. The Hall-voltage E_{H1} can be written as the vector product

$$E_{H1} = R_H \ (B_1 \ \cos \ \omega t \ \times \ J) \tag{5.3}$$

The Hall-coefficient R_H is characteristic of the semi-conducting ma- **69**

terial. For more information on the Hall-effect we refer to refs. (30) and (31).

In our equipment we use the effect by introducing the displacement signal $y_1 \cos (\omega t - \phi)$ as control current through the probe. Thus, Eq. (5.3) yields the integrand of Eq. (5.1) apart from supplying a scale factor. Starting from a magnetic-induction vector $B_1 \sin \omega t$ (see Sec. 5.2.1, Hall-probe 2), we work out the integrand of Eq.
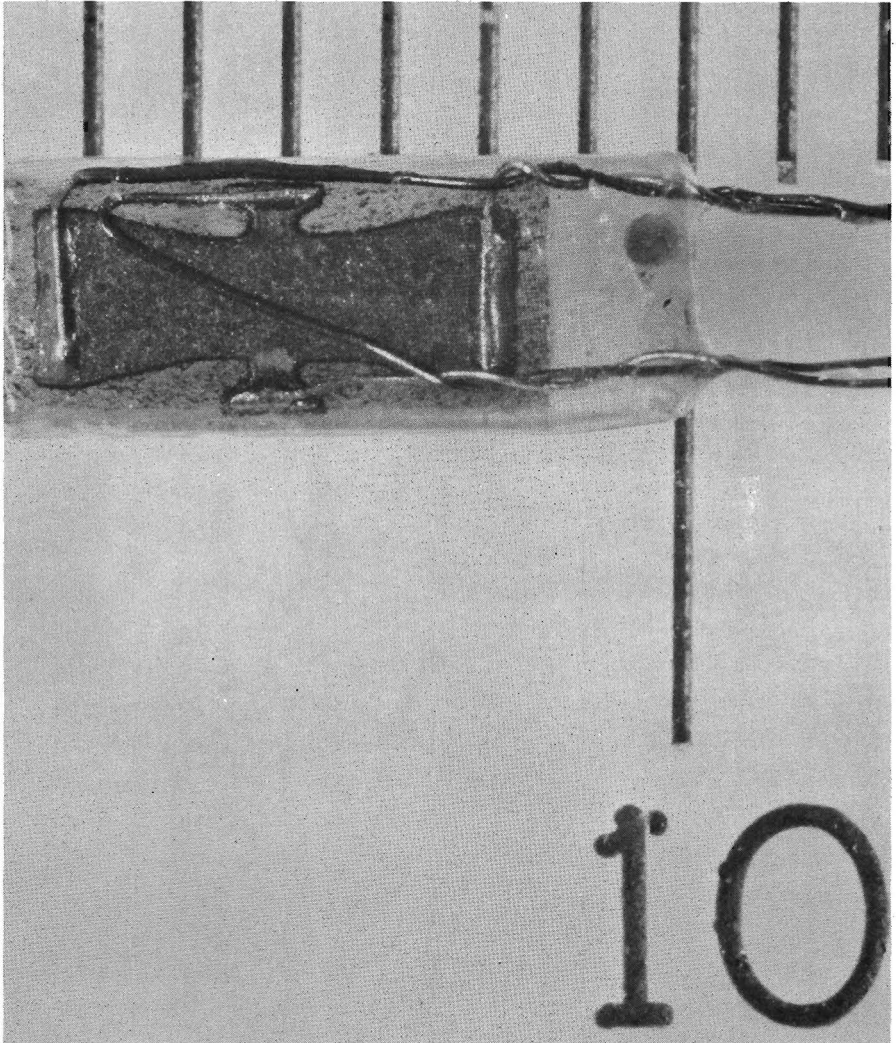
Fig.5.5. The Hall-probe

(5.2). The constant part of the magnetic induction B_0 has found to be ineffective with respect to the Eqs. (5.1) and (5.2) and, consequently, has been ignored in the preceding pages of this section.

The Hall-probes (Siemens) used in our equipment have small dimensions (7 x 3.2 x 0.5 mm^3). Fig. 5.5 shows a photograph of such a probe.
In it we can distinguish the connections for control current and Hall-voltage.

The multiplication properties of the Hall-probes are checked in the following way. The probes are controlled by direct current, while the magnetic field is kept constant (piston is stopped).
Thus, the quotient of control current and Hall-voltage ought to be constant in the operating range of the control current (25 ÷ 150 mA). For one measuring series we chose six different values of the control current. Then the standard deviation of the quotient mentioned is determined. The investigation has been carried out for both the maximum and the minimum air gap. Table 5.1 shows the results.

	air gap	standard deviation %
Hall-probe 1	min.	1.8
Hall-probe 1	max.	1.2
Hall-probe 2	min.	1.1
Hall-probe 2	max.	1.4

Table 5.1. Results of the multiplication check of the Hall-probes

The results are highly acceptable for our purpose, the more so as the accuracy of the instruments used with the experiments, is incorporated in the results. Furthermore, we have checked the phase angle between the two Hall-signals when the piston rotates.

Therefore, the control current has been kept constant again. Thus, the phase angle between E_{H1} and E_{H2} ought to be $\pi/2$ rad. With the aid of a phase-angle meter (Peekel) we found that this was correct within ± 0.02 rad.

5.2.3. The problem of the time delay

Fig. 5.6 shows diagrammatically our equipment for plotting Nyquist-curves.
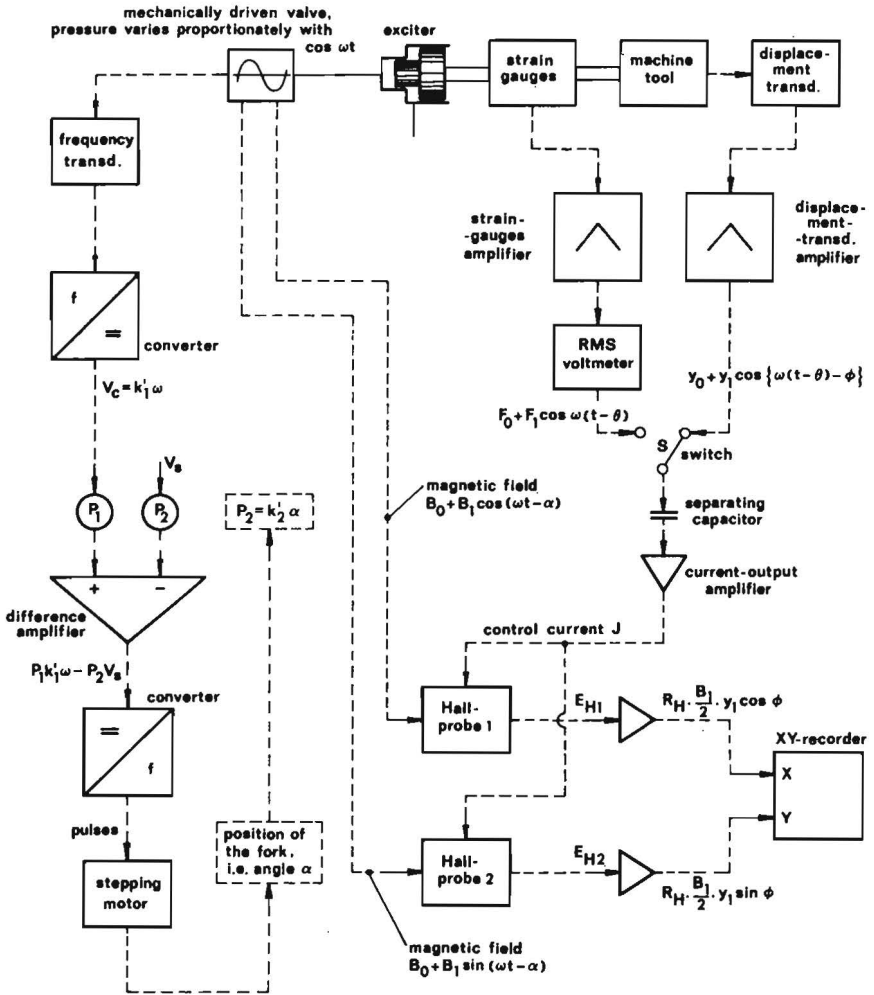

Fig.5.6. The complete equipment

In this figure we have assumed that the oil pressure in the mechani-
cally driven valve varies proportionately with cos ωt. The force sig-
nal from the strain-gauges amplifier (Hottinger) has a time delay θ
with respect to the pressure signal mentioned, which results in a

phase angle $\omega.\theta$ between the two signals. The phase angle between the output of the strain-gauges amplifier and the output of the displacement-transducer amplifier (Hottinger) is assumed to be ϕ. This angle is introduced by the dynamic properties of the machine tool.

Furthermore, we have assumed that in fig. 5.6 the magnetic fields for the Hall-probes 1 and 2 have a delay with respect to the pressure signal in the valve over α and $(\alpha + \pi/2)$ rad respectively. The angle α characterises the position of the fork (see Sec. 5.2.1) and can be changed with the aid of a servo system, in which a stepping motor drives the fork.

For correct plotting of the Nyquist-curve of the machine tool to be investigated, it is necessary that the following relation exists

$$\alpha = \omega\theta \qquad\qquad\qquad (5.4)$$

First of all we have to answer the question whether the time delay θ depends on the frequency or not. Therefore, the phase angle between the output signal of the strain-gauges amplifier and the Hall-voltage E_{H1} as a reference signal was measured in a number of frequency ranges. For this purpose, Hall-probe 1 was controlled with direct current. As to the lengths of pipes we took the same configuration as used during the measurements for the Bode-diagram of the control system (see Sec. 4.2). Before starting the measurements in a frequency range, the fork was placed in such a position that in the middle of the range in question the phase angle $\omega.\theta$ between the two above signals was zero. After that, the position of the fork was not changed anymore. The results of the measurements in two ranges are shown in fig. 5.7.

The results show that the phase angle is proportional to the frequency. The gradient of both curves is the same and correspondends to the time delay θ. Measuring of this gradient yields $\theta = 1.62$ ms, of which 0.33 ms should be imputed to the strain-gauges amplifier according to the statement of its manufacturer. Hence, the angle α should be proportional to ω. This is basic for the servo system which controls the position of the fork (see fig. 5.6).

Potentiometer P_1 and supply voltage V_s are adjustable.
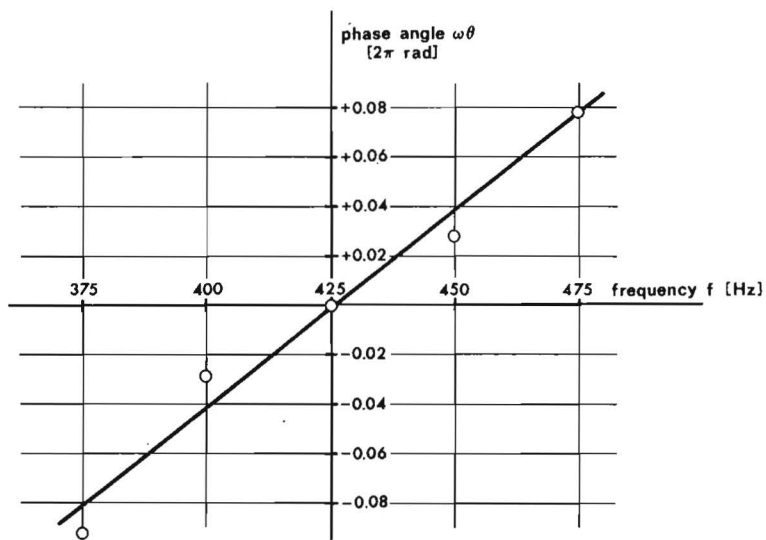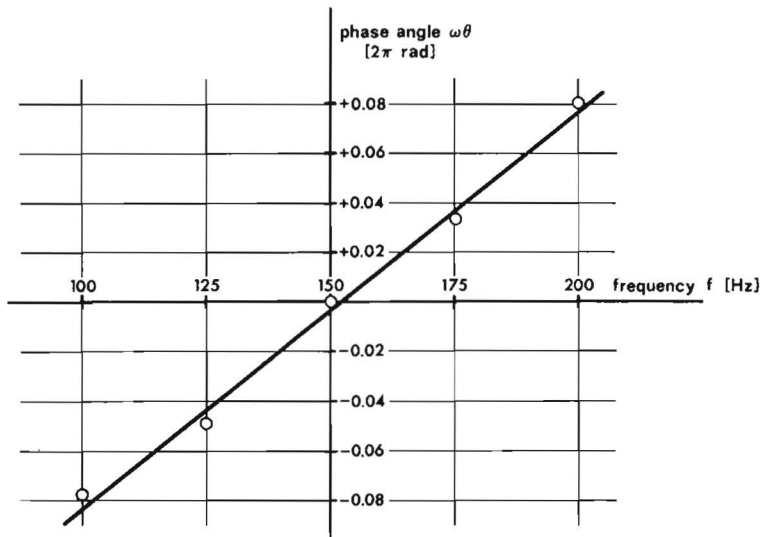Potentiometer P_2 indicates the position of the fork (potentiometer F **73**

Fig.5.7. Phase angle $\omega.\theta$ between force signal and E_{H1} as a function
of frequency f

in fig. 5.2, see Sec. 5.2.1). We adjust the system in such a way that
$\alpha = 0$ for $\omega = 0$ and that the following relation is valid

$$P_2 = k_2' \, \alpha \qquad\qquad (5.5)$$

The difference amplifier which drives the converter for the stepping

motor has two input signals, viz. a signal proportional to the frequency ($P_1 . k'_1 . \omega$) and a signal ($P_2 . V_s$) proportional to the angle α as can easily be seen with Eq. (5.5). If the stepping motor is at rest, the two signals must be equal to each other. Thus, we find, using Eq. (5.5)

$$\alpha = \frac{P_1 \, k'_1}{V_s \, k'_2} \, \omega \qquad\qquad (5.6)$$

Eqs. (5.4) and (5.6) yield

$$\theta = \frac{P_1 \, k'_1}{V_s \, k'_2} \qquad\qquad (5.7)$$

In other words, the servo system can be adjusted with the aid of P_1 and V_s. It should be remarked that it is not necessary to know the value of θ precisely for adjusting P_1 and V_s. There is an easier way to check whether P_1 and V_s are correctly adjusted.

To this end, we connect the strain-gauges amplifier to the current-output amplifier by means of switch S. As can be seen in fig. 5.6, the latter amplifier can only be operated by dynamic signals, due to the presence of the separating capacitor. With a well-calibrated equipment, the XY-recorder has to mark point 2 in fig. 5.8. However, P_1 and V_s generally have arbitrary values. So let us assume that point 1 corresponds with these values.
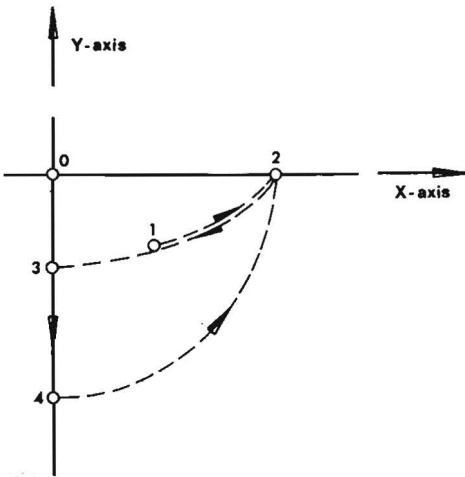
Fig.5.8. Calibration of the XY-recorder

Next, we vary P_1 (or V_s) in such a way that the point in the XY-plane comes on the X-axis (point 2). With similar integrals as used in Eqs. (5.1) and (5.2), it is easy to prove that now the correct value for θ has been adjusted. Variation of P_1 (or V_s) has the same effect of introducing extra time-delay, i.e. phase variation without effecting
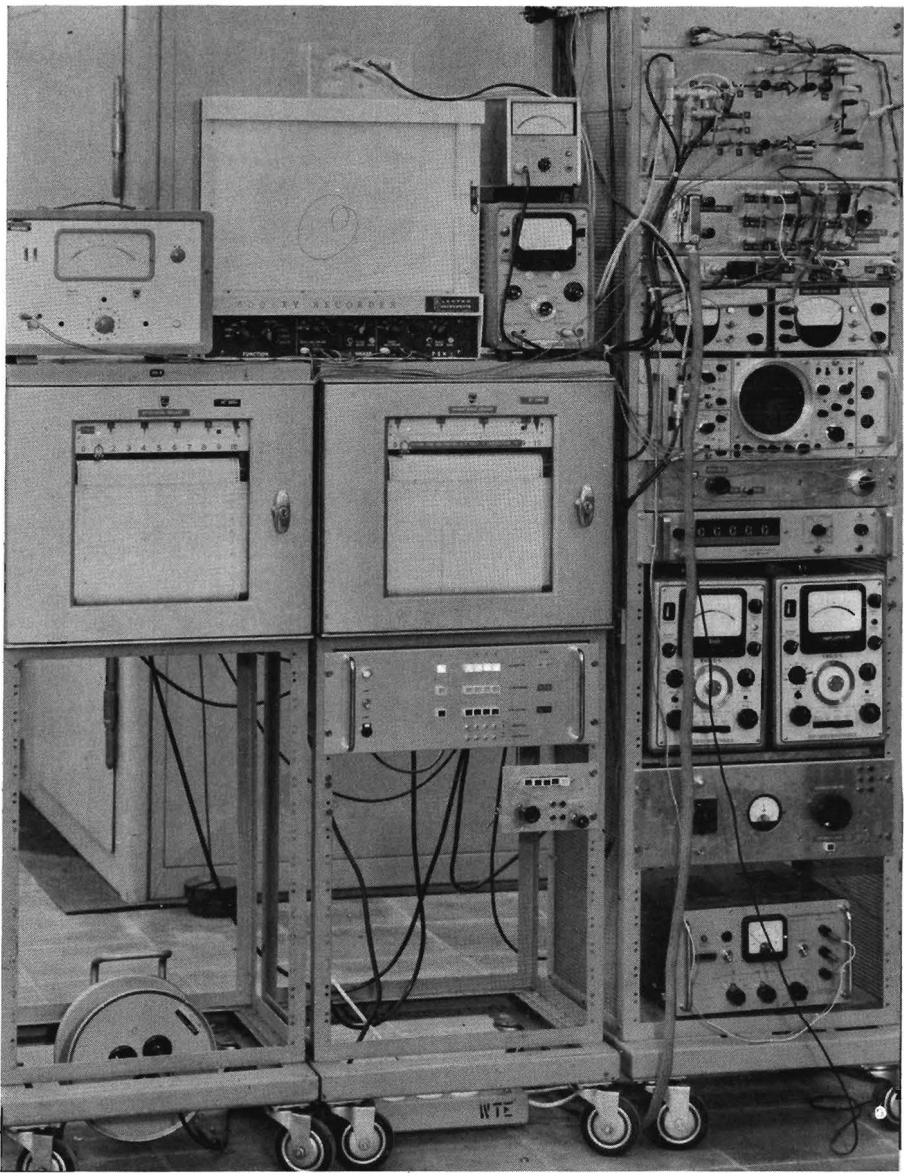
Fig.5.9. Electronic equipment

the amplitude. If we switch over from point 2 to point 3 by means of
a variation of P_1 (or V_s) we can check whether the distance 02 is e-
qual to the distance 03 or not. In the latter case, scale variation
of the Y-axis leads to point 4 lying at the same distance from the
origin as point 2. Now, we can calibrate the axes of the recorder

Fig.5.10. Detail photograph of drill, exciter, and table

with the RMS-voltmeter. We then return to point 2. After reversion
of switch S, the machine tool is inserted into the calibrated measu-
ring-chain. If, in addition, both strain-gauges amplifier and dis-
placement-transducer amplifier have the same time-delay, the equip-
ment is ready for plotting the Nyquist-curve of the machine tool.
Fig. 5.9 shows a photograph of the electronic equipment.
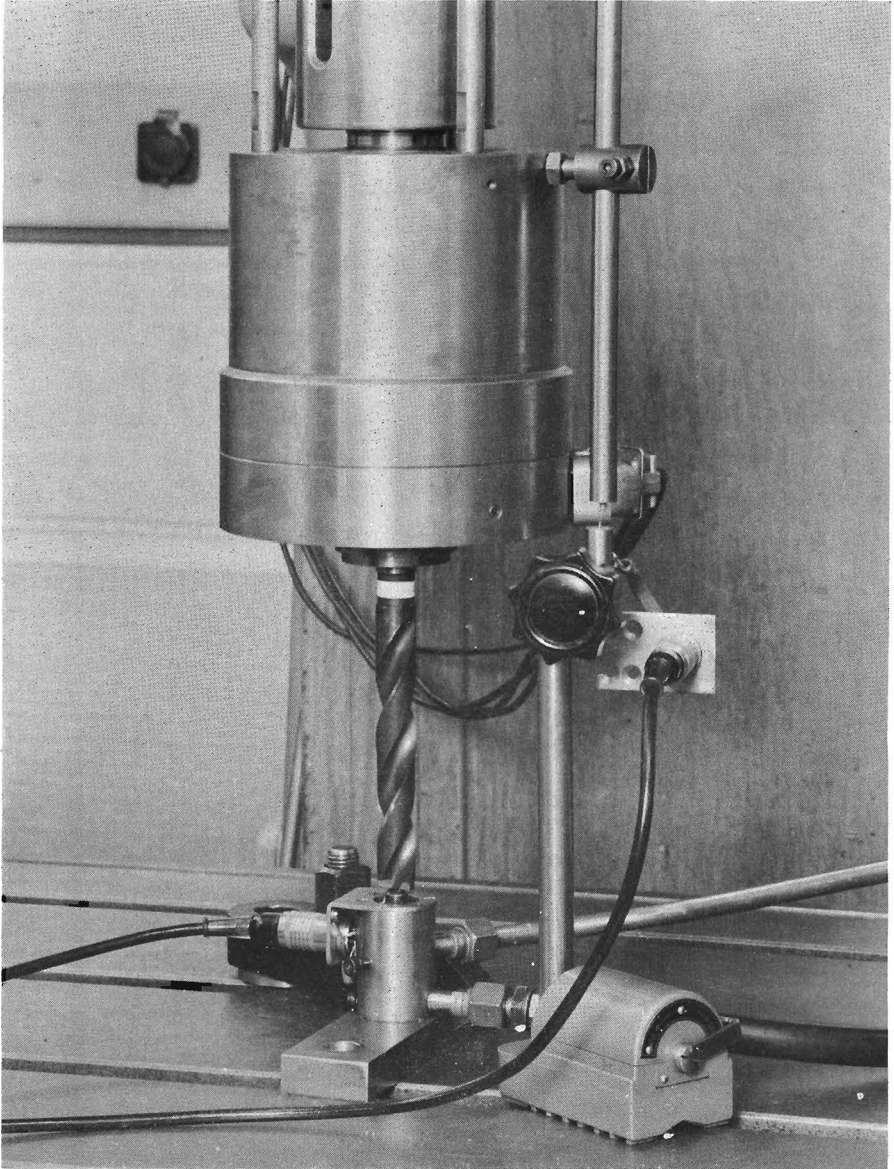

5.3. An application

The usefulness of the equipment described in the foregoing sections
was tested on an experimental drilling-machine (Hettner). The same
machine tool also came up for discussion in Sec. 4.3. The exciter is
placed once more between drill (in dynamometer) and table, as can be
seen in fig. 5.10.
From the position of the exciter it can be seen that the machine tool
is excited in axis direction of the drill.
A former investigation of this machine tool yielded some natural fre-
quencies in the range from 350 up to 410 Hz. Therefore, we have in-
vestigated this drilling machine in that particular range. The cali-
bration of the equipment, as described in the last part of the pre-
vious section, was carried out at about 380 Hz.
Fig. 5.11 shows the Nyquist-diagram of the drilling machine for a sta-
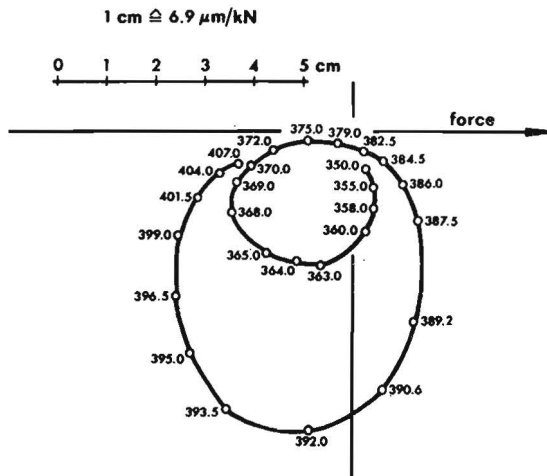
78 Fig.5.11. Nyquist-diagram for F_0 = 1390 N and F_1 = 108 N

tic force F_0 = 1390 N and a dynamic force with amplitude F_1 = 108 N.
We readily see two natural frequencies, viz. 365 Hz and 392 Hz. The
displacement amplitude measured between dynamometer and table is
2.3 µm for 365 Hz and 4.6 µm for 392 Hz.

In order to get an impression of the reproducibility of the equipment,
the entire experiment was repeated. However, before starting this
second experiment, the equipment was first brought out of adjustment
and then again calibrated on another scale. Passing through the above-
mentioned frequency-range, we found the curve of fig. 5.12.

1 cm ≙ 4.6 µm/kN
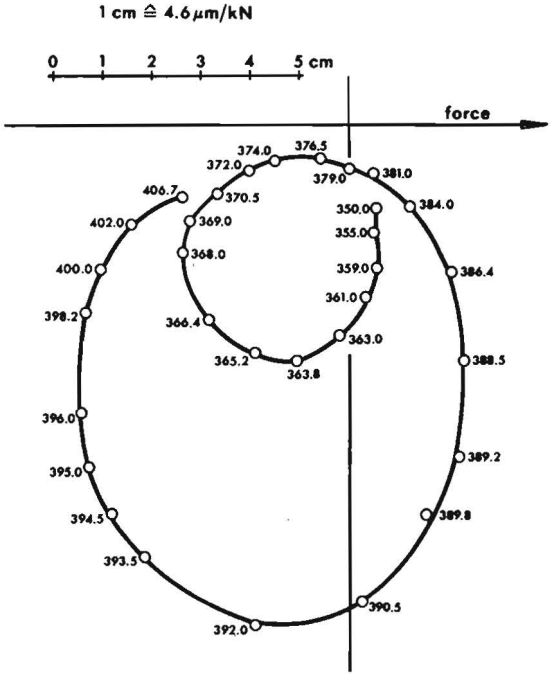
Fig.5.12. Nyquist-diagram for F_0 = 1360 N and F_1 = 103 N

Both the static and dynamic force is approximately the same as in
the previous experiment. As displacement amplitudes at 365 Hz and
392 Hz we now find 2.4 µm and 4.8 µm respectively. We may establish a
rather good similarity between the curve of fig. 5.11 and that of
fig. 5.12.

In this context we like to make some remarks about disturbance in-
fluences and accuracies of the equipment in as far as they have not   **79**

been mentioned in the foregoing. External interferences penetrating into the system through the displacement transducer, are attenuated by means of integrating filters at the inputs of the XY-recorder. As to the calibration of the axes of the recorder, we estimate the accuracy of the resulting scale-value at 3.8 %. The accuracy of the displacement measurement, of the RMS-voltmeter, the multiplication, the amplifiers, and the XY-recorder are all worked up in this calibration accuracy. During the experiments we are to calculate with a measurement accuracy of 2.2 % as well. So we find a total accuracy of 4.3 % for one axis.

So far, we have ignored an important aspect, viz. the accuracy with which the servo system solves the time-delay problem. We can check the operation of this system during the experiments by simply reversing the switch S (see fig. 5.6) for a moment, which implies that the recorder is to write point 2 on the X-axis (see fig. 5.8). During the foregoing experiments we did this several times. The points thus found were always situated within a circle around point 2 with a radius of 10 % of the distance 02. Needless to say that in this way we

1 cm ≙ 4.9 μm/kN
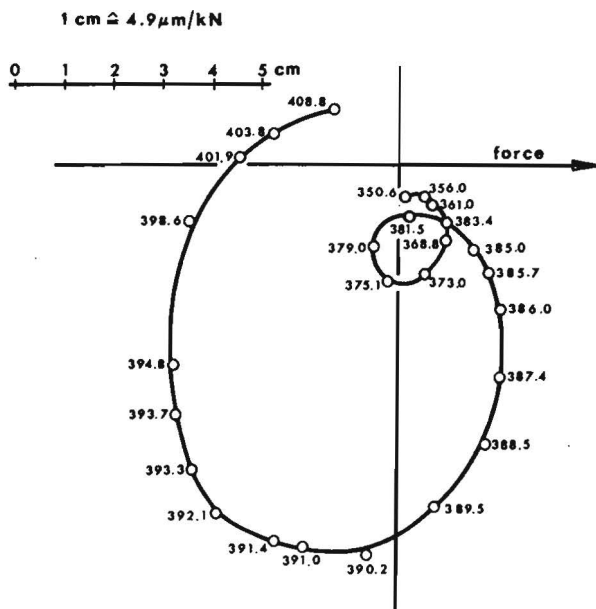
Fig.5.13. Nyquist-diagram for F_0 = 1066 N and F_1 = 104 N

have also checked the operation of the control system described in
Chap. 4.

Fig. 5.13 shows another Nyquist-curve of the drilling machine. The
static force was decreased by about 22 % with respect to the fore-
going values. The dynamic force was kept practically unchanged.
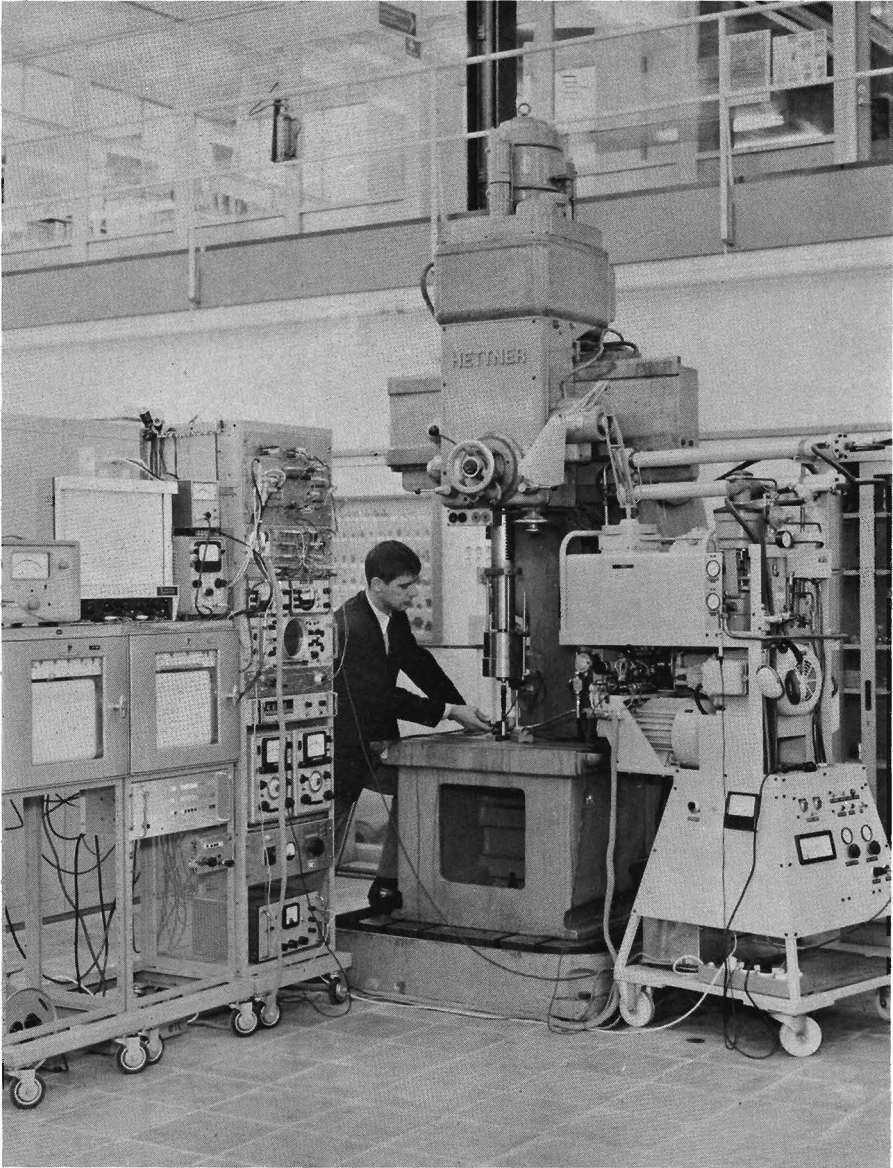
Fig.5.14. The total plant

We can now observe a clear change in the curve. Especially, the magnitude and the position of the smallest loop are quite different from those in the previous curves. This gives us the information that the machine tool consists of non-linear elements. It will be clear that dynamic investigation of such kind of machine tools by means of electro-dynamic exciters can only be evaluated to a rather limited extent. We will close this chapter with a photograph of the total plant (fig. 5.14).

CONCLUSIONS

We may establish that the purpose set out in the first chapter, viz.
the designing of an exciter for dynamic investigation of machine
tools, is attained. In spite of the restrictions the hydraulic sytem
imposes on us with respect to the transport of dynamic pressure-
signals, it has turned out to be possible to generate exciter forces
that are in the same order of magnitude as the cutting forces of
medium-type machine tools. A control system, as discussed in Chap. 4,
appeared to be an indispensable aid to guarantee a certain constancy
of the exciter forces. The usefulness of the equipment could probably
be increased by the application of valves with linear characteristics
in this control system. The method used for recording the transfer
function of the machine tool worked out to our entire satisfaction
during the investigation of the experimental drilling-machine.
Although the polar diagram can continuously be recorded by the equip-
ment described, we abstained from such facility for practical reasons.
In conclusion, we express our hope that the exciter, as the gist of
this thesis, may lead to a further insight into the dynamic behaviour
of machine tools during the cutting process.

TABLE OF SYMBOLS

P	cutting force	N
k_1	chip-thickness coefficient	N/mm
s	chip thickness	mm
k_2	penetration coefficient	N.s/mm
r	feed rate	mm/s
k_3	cutting-speed coefficient	N.s/m
v	cutting speed	m/s
k'	cutting-force coefficient	N/mm
t	time	s
T	time	s
x_t	position of tool at time t	mm
x_{t-T}	position of tool at time (t-T)	mm
μ	overlapping coefficient	--
Q	rate of flow	m^3/s
p	pressure	N/m^2
V	voltage	V
V_{ref}	voltage	V
i	current	A
i_{max}	current	A
t_1	time	s
C	discharge coefficient	--
A	area	m^2
Δp	pressure drop across valve orifice	N/m^2

84

ρ	density of fluid medium	kg/m^3
b_n	coefficient of the Fourier series	N/m^2
ω	angular velocity	s^{-1}
A_{stat}	area	m^2
A_{dyn}	area	m^2
f	frequency	s^{-1}
v	velocity	m/s
x	distance along pipe	m
E	modulus of elasticity	N/m^2
Δx	length of pipe segment	m
p_k	pressure at point x_k	N/m^2
v_k	velocity at point x_k	m/s
p_m	maximum value of pressure	N/m^2
v_m	maximum value of velocity	m/s
p_k^*	dimensionless pressure at point x_k	--
v_k^*	dimensionless velocity at point x_k	--
τ	computer time	s
β	time scale factor	--
C_1	coefficient defined in Eq. (3.8)	s^{-1}
C_2	coefficient defined in Eq. (3.9)	s^{-1}
C_3	coefficient defined in Eq. (3.14)	--
C_4	coefficient defined in Eq. (3.15)	--
A_n	coefficient of the Fourier series	m^2
C_5	coefficient defined in Eq. (3.21)	--
C_6	coefficient defined in Eq. (3.22)	--
C_7	coefficient defined in Eq. (3.23)	--
C_8	coefficient defined in Eq. (3.24)	--
C_9	coefficient defined in Eq. (3.25)	--

|		
C_{10}	coefficient defined in Eq. (3.26)	s^{-1}
$\Delta x'$	length of pipe segment in pipe 2 [*]	m
$\Delta x''$	length of pipe segment in pipe 3	m
z	coordinate describing the position of M	m
M	mass	kg
D	damping constant	N.s/m
K	spring constant	N/m
A_e	area of exciter piston	m^2
A_p	cross-sectional area of pipe	m^2
z_m	maximum value of z	m
$\dot{z}_m$	maximum value of $\dot{z}$	m/s
C_{11}	coefficient defined in Eq. (3.49)	s^{-1}
C_{12}	coefficient defined in Eq. (3.50)	s^{-1}
C_{13}	coefficient defined in Eq. (3.51)	s^{-1}
C_{14}	coefficient defined in Eq. (3.53)	s^{-1}
C_{15}	coefficient defined in Eq. (3.55)	--
l_1	length of pipe 1 (see fig. 3.16)	m
l_2	length of pipe 2	m
l_3	length of pipe 3	m
ω_0	angular velocity defined in Eq. (3.56)	s^{-1}
q	amplification factor defined in Eq. (3.57)	--
z_0	maximum displacement-amplitude of M	m
F_1	force amplitude	N
y_1	displacement amplitude	m
ϕ	phase angle	--

[*] The variables in pipes 1, 2 and 3 (see fig. 3.16) are distinguished from each other by means of accent marks.

|		
B_1	amplitude of magnetic induction	$V.s/m^2$
B_0	constant part of magnetic induction	$V.s/m^2$
E_{H1}	Hall-voltage of probe 1	V
E_{H2}	Hall-voltage of probe 2	V
J	current density	A/m^2
R_H	Hall-coefficient	$m^4/A.s$
F_0	static force	N
y_0	static displacement	m
θ	time delay	s
α	position of fork, phase angle	--
P_1	position of potentiometer	--
P_2	position of potentiometer	--
V_c	converter voltage	V
k'_1	coefficient	V.s
V_s	supply voltage	V
k'_2	coefficient defined in Eq. (5.5)	--

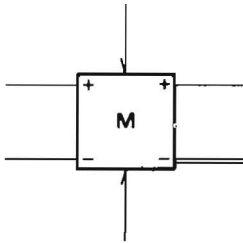## TABLE OF ANALOGUE-COMPUTER SYMBOLS

 potentiometer
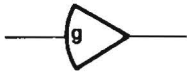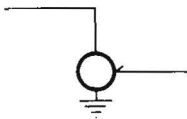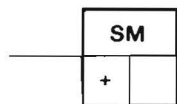
 operational amplifier

 summing amplifier
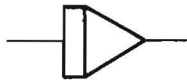
 integrating amplifier

 multiplier

 servo potentiometer

 servo multiplier

REFERENCES

(1) ARNOLD, R.N.: The mechanism of tool vibration in the cutting of steel. Proceedings Institution of Mechanical Engineers 154 (1946).

(2) HAHN, R.S.: Metal cutting chatter and its elimination. Transactions of the A.S.M.E. 75 (1953).

(3) DOI, S. and KATO, S.: Chatter vibration of lathe tools. Transactions of the A.S.M.E. 78 (1956).

(4) TOBIAS, S.A. und FISHWICK, W.: Eine Theorie des regenerativen Ratterns an Werkzeugmaschinen. Der Maschinenmarkt, (13a) Coburg – Nr. 17 –, 28. Februar 1956.

(5) TOBIAS, S.A.: Schwingungen an Werkzeugmaschinen. Hanser Verlag, München 1961.

(6) TLUSTY, J., POLACEK, M., DANEK, O., SPACEK, L.: Selbsterregte Schwingungen an Werkzeugmaschinen. V.E.B. Verlag Technik, Berlin 1962.

(7) PETERS, J. und VANHERCK, P.: Ein Kriterium für die dynamische Stabilität von Werkzeugmaschinen. Industrie-Anzeiger, Essen Nr. 11 – 5. Februar 1963 and Nr. 19 – 5. März 1963.

(8) TLUSTY, J., POLACEK, M.,: Beispiele der Behandlung der selbsterregten Schwingungen der Werkzeugmaschinen. 3.FoKoMa, Vogel Verlag, Coburg 1957.

(9) GURNEY, J.P. and TOBIAS, S.A.: A graphical method for the determination of the dynamic instability of machine tools. International Journal of Machine Tool Design and Research Vol. 1 (1961).

(10) LEMON, J.R. and LONG, G.W.: Survey of chatter research at the Cincinnati Milling Machine Company. Proceedings of the fifth International M.T.D.R. Conference University of Birmingham, September 1964.

(11) TOBIAS, S.A.: Machine tool vibration. Blackie & Son, Glasgow 1965, p. 331.

(12) GEIGER, H.G.: Statische und dynamische Untersuchungen an Schwer-
werkzeugmaschinen. Dissertation T.H. Aachen 1965.

(13) KOENIGSBERGER, F., PETERS, J. and OPITZ, H.: Report of the Working
Group Ma. Annals of the C.I.R.P. Vol. XIV 1966.

(14) REHLING, E.R.: Entwicklung und Anwendung elektro-hydraulischer
Wechselkrafterreger zur Untersuchung von Werkzeugmaschinen. Dis-
sertation T.H. Aachen 1965.

(15) RIEMER, G. e.a.: Handboek voor landbouwwerktuigen en trekkers.
Dl. II Tjeenk Willink, Zwolle 1961.

(16) KRAAKMAN, H.J.J.: Hydraulische vermoeiïngsinrichting. Octrooiaan-
vrage No. 6404150, 16 april 1964.

(17) OSTERMANN, H.: Moderne Antriebe mit Thyristoren. De Ingenieur,
16 april 1965.

(18) WOLF, A.C.H. VAN DER, BEER, C. DE: Ein hydraulischer Erreger
für die dynamische Untersuchung von Werkzeugmaschinen. Industrie-
Anzeiger, Essen Nr. 76 - 23. September 1966.

(19) ROGERS, A.E., CONNOLLY, T.W.: Analog computation in enginee-
ring design. McGraw-Hill Book Company, Inc., New York 1960.

(20) JACKSON, A.S.: Analog computation. McGraw-Hill Book Company, Inc.
New York 1960.

(21) BLACKBURN, J.F., REETHOF, G., SHEARER, J.L.: Fluid power con-
trol. Published jointly by The Technology Press of M.I.T. and
John Wiley & Sons, Inc., New York and London 1960.

(22) BINDER, R.C.: Advanced fluid dynamics and fluid machinery. Pren-
tice-Hall, Inc., Englewood Cliffs, N.J. 1957.

(23) SHAPIRO, A.H.: The dynamics and thermodynamics of compressible
fluid flow. Vol. II. The Ronald Press Company, New York 1953.

(24) KUIPERS, L., TIMMAN, R.: Handboek der Wiskunde. Scheltema &
Holkema N.V., Amsterdam 1963, p. 512.

(25) SCHLÖSSER, W.M.J.: Meten aan verdringerpompen. Proefschrift T.H.
Delft 1959.

(26) VIERSMA, T.J.: Investigations into the accuracy of hydraulic ser-
vomotors. Doctor's thesis Technological University Delft 1961,
p. 85.

(27) PETERS, J.: Damping in machine tool construction. Proceedings of
the sixth International M.T.D.R. Conference The Manchester Colle-
ge of Science & Technology, September 1965, p. 25.

(28) LANDBERG, P.: Gebruik en behandeling van snelstalen spiraalboren
     op radiaalboormachines in enige Nederlandse fabrieken II. Metaal-
     bewerking, 29 oktober 1959, p. 174.

(29) BASEL, C. VON und ZANTEN, M. VAN: Messung gerichteter mechanischer
     Schwingzeigergrössen zur Aufzeichnung von Ortskurven. Archiv für
     Technisches Messen, V 171 - 6 Lieferung 305, Juni 1961 and
     V 171 - 7 Lieferung 306, Juli 1961.

(30) BEER, A.C.: The Hall effect. International Science and Technology,
     No. 60, december 1966.

(31) KRONIG, R. e.a.: Leerboek der natuurkunde.
     Scheltema & Holkema N.V., Amsterdam 1958, p. 575.

SAMENVATTING

Het onderwerp van dit proefschrift is de ontwikkeling van apparatuur
voor het dynamisch onderzoek van gereedschapswerktuigen. In het eer-
ste hoofdstuk worden de theorieën over zelf-opgewekte trillingen
tijdens het verspaningsproces kort aangeduid. Tegen de achtergrond
van deze theorieën worden in dit hoofdstuk tevens de eisen aangegeven
waaraan de hydraulische excitator, als voornaamste onderdeel van ge-
noemde apparatuur, dient te voldoen. In het volgende hoofdstuk worden
de belangrijkste onderdelen van de apparatuur besproken. Behalve aan
de constructie, wordt ook aandacht geschonken aan de fysische groot-
heden welke een rol spelen. Bij enkele onderdelen is het verband tus-
sen deze grootheden op experimentele wijze bepaald. Hoofdstuk 3 is
geheel gewijd aan modelstudie met behulp van een analoge rekenmachine.
Allereerst wordt door vergelijking van resultaten van een vereenvou-
digd model van de proefopstelling (model A) en resultaten afkomstig
van experimenten in het laboratorium aangetoond dat een dergelijke
modelstudie geoorloofd is. Daarna wordt met model B, dat meer overeen-
komt met de werkelijke proefopstelling, de mogelijkheden en grenzen
van de apparatuur aangegeven. Uit deze laatste studie blijkt o.a. de
noodzaak van een regelsysteem voor het constant houden van de excita-
torkracht. Dit regelsysteem wordt in hoofdstuk 4 besproken. Tenslotte
wordt in het laatste hoofdstuk een methode voor het schrijven van
Nyquist-diagrammen van een gereedschapswerktuig uiteengezet. Hierbij
wordt gebruik gemaakt van Hall-generatoren. Het hoofdstuk wordt be-
sloten met enkele resultaten van een dynamisch onderzoek aan een ex-
perimentele boormachine.

CURRICULUM VITAE

De schrijver van dit proefschrift werd in 1935 te Breda geboren.
Hij bezocht aldaar het Onze Lieve Vrouwe Lyceum, waar hij in 1954
het diploma HBS-B behaalde. Daarna volgde hij onderwijs aan de
Hogere Technische School St. Virgilius te Breda, alwaar hij in 1957
het examen van de afdeling werktuigbouwkunde met goed gevolg aflegde.
Van 1957 tot 1959 vervulde hij zijn militaire dienstplicht. Tijdens
deze periode kreeg hij een opleiding tot radarofficier en was als
zodanig werkzaam bij een afdeling luchtdoelartillerie.
In 1959 begon hij zijn studie aan de Technische Hogeschool te Eind-
hoven; in 1964 verwierf hij daar het diploma van werktuigkundig in-
genieur. Sinds augustus 1961 is hij als medewerker verbonden aan het
Laboratorium voor Mechanische Technologie en Werkplaatstechniek van
eerder genoemde hogeschool. In deze functie vond hij de gelegenheid
het onderhavige proefschrift te bewerken.

STELLINGEN

I

E.R. Rehling maakt de methodologische fout dat hij zijn werkhypothese omtrent de niet-samendrukbaarheid van olie, in zijn conclusies gehanteerd heeft als een feitelijke en niet geverifieerde waarheid.

> E.R. Rehling, Entwicklung und Anwendung elektro-hydraulischer Wechselkrafterreger zur Untersuchung von Werkzeugmaschinen.
> Dissertation T.H. Aachen 1965, p. 32, e.v.

II

Ten onrechte worden de mogelijkheden welke de analoge rekenmachine biedt bij de analyse van dynamica problemen achtergesteld bij die van de digitale rekentechnieken.

III

De vanzelfsprekendheid waarmee op een analoge rekenmachine differentiemethoden ter bepaling van eerste afgeleiden worden toegepast in het geval dat het gebied van de onafhankelijk veranderlijke is opgedeeld in gelijke intervallen, werkt remmend op de toepassing van deze methoden wanneer genoemde intervallen niet gelijk zijn.

IV

Een correcte invoering van het SI-eenhedenstelsel bij het technisch onderwijs wordt in niet geringe mate belemmerd door het feit dat de numerieke waarde van de versnelling van de zwaartekracht op aarde (ongeveer 9,8 m/s^2) slechts weinig afwijkt van het getal 10.

V

Het is wenselijk in het elektronica-onderwijs het accent te verleggen van onderricht in de werking van discrete onderdelen naar dat van geïntegreerde systemen.

VI

Een aantal van de argumenten die door een minderheid van de "commis-
sie-Verdam" tegen de door de werknemers te benoemen commissaris wor-
den aangevoerd, is weinig relevant.

> Herziening van het ondernemingsrecht.
> Rapport van de Commissie ingesteld bij beschikking van de
> Minister van Justitie van 8 april 1960.
> Staatsuitgeverij, 's-Gravenhage 1965, p. 21, e.v., p. 101,
> e.v.

VII

Bij het ontwerpen van opnemers voor het meten van fysische groothe-
den verdient de methode waarbij de betrokken grootheid rechtstreeks
wordt omgezet in een tijdgrootheid, meer de aandacht.

> A better weigh.
> Electronics, december 11, 1967, p. 255.

VIII

Internationale samenwerking op technisch gebied dient gericht te zijn
op het welzijn van alle betrokken volken; derhalve is het stellen van
beperkende voorwaarden ten gunste van slechts nationale belangen in
dezen onbehoorlijk.

IX

Het verdient aanbeveling bij de adressering van poststukken de
plaatsnaam en de naam van de geadresseerde ook in deze rangorde te
geven.

Eindhoven, 22 maart 1968   A.C.H. van der Wolf